

**EXPERIMENTAL AND ANALYTICAL STUDY OF THE DESIGN
OF REINFORCEMENT IN
FOLDED PLATES AND CYLINDRICAL SHELL STRUCTURES**

52
CE
1971
M
SIN
EXP

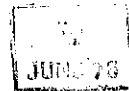
**EXPERIMENTAL AND ANALYTICAL STUDY OF THE DESIGN OF
REINFORCEMENT IN FOLDED PLATES AND CYLINDRICAL SHELL STRUCTURES**

A Thesis Submitted

In Partial Fulfilment of the Requirements

for the Degree of

MASTER OF TECHNOLOGY



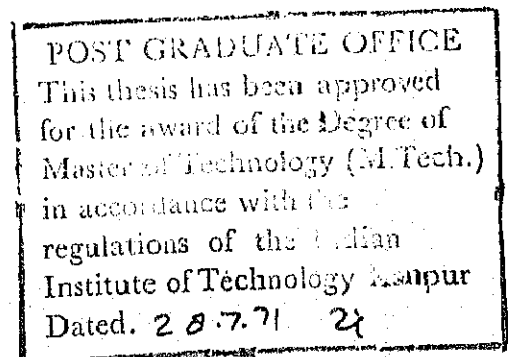
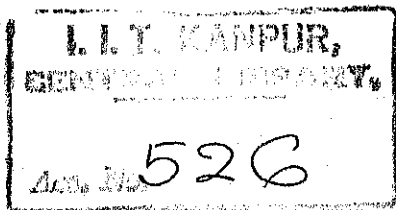
Thesis

by

624.1776

LAL SINGH

Sl 64 e



to the

CE-1971-M-SIN-EXP

DEPARTMENT OF CIVIL ENGINEERING

INDIAN INSTITUTE OF TECHNOLOGY KANPUR

JULY 1971

CERTIFICATE

This is to certify that the work entitled
' EXPERIMENTAL AND ANALYTICAL STUDY OF THE DESIGN OF REINFORCEMENT
IN FOLDED PLATES AND CYLINDRICAL SHELL STRUCTURES' by Lal Singh
has been carried out under my supervision and has not been submitted elsewhere for a degree.

A. V. Setlur

(A. V. Setlur)
Assistant Professor
Department of Civil Engineering
Indian Institute of Technology,
Kanpur.

Dated: July, 1971.

POST GRADUATE OFFICE
This thesis has been approved
for the award of the Degree of
Master of Technology (M.Tech.)
in accordance with the
regulations of the Indian
Institute of Technology Kanpur
Dated. 28.7.71 28

ACKNOWLEDGEMENTS

I wish to express indebtedness to Dr. A. V. Setlur for suggesting the topic of thesis and his encouraging guidance throughout the progress of work.

I am thankful to Dr. P. Dayaratnam for his valuable suggestions in the experimental work.

I express my thankfulness to Dr. J.K. Sridhar Rao for making available some of the references.

Thanks are due to

- 1) Staff of structural laboratory for their help throughout the experiment.
- 2) Computer Centre for using IBM 7044 and IBM 1401.

Thanks to Mr. V. Rajaman for his help in drawing work.

Thanks to Shri R. K. Jain for his excellent typing.

LAL SINGH

To

MY BIG BROTHER

SYNOPSIS

The conventional methods of design of folded plates and cylindrical shell structures need the reinforcement to be placed along arbitrary space curves which is a cumbersome task. Therefore, the necessity of an easier method is felt. ACI Code has given some principles for the layout of an orthogonal reinforcement.

A rational method to design an orthogonal reinforcement in folded plate structures is (a) to calculate the modified stresses termed as design-stresses in two coordinate directions at top, middle and bottom of the assumed thickness by adding absolute values of shear stresses to the net stresses, the later being obtained by algebraic sum of membrane and bending stresses. (b) to calculate the reinforcement for upper half thickness for the mean-value of design-stresses at top and middle and for lower half thickness for the mean value of design stresses at middle and bottom of thickness. This method has been experimentally verified and found safe.

To overcome the intricacy of layout of reinforcement in cylindrical shell structures, a new method of design is to divide the shell surface into different regions according to the load-dispersion directions and then to calculate the reinforcement in strips along those load-dispersion directions. This method needs to be verified experimentally as well as theoretically by computing the ultimate capacity of a cylindrical shell structure designed as above, by yield line theory.

CONTENTS

CHAPTER I : INTRODUCTION	1
1.1 A brief history of the evolution of the methods of analysis and design of the folded plate structures.	1
1.2 Aim of the present study.	4
1.2.1 Experimental Verification of the proposed Method of Design of Folded Plate Structures.	4
1.2.2 Comparison Of the Experimental Results with the Existing Ultimate Load Theories of Folded Plate Structures.	4
1.2.3 Proposition of a New Approach For The Design of Folded Plates and Cylindrical Shell Structures.	4
CHAPTER II : EXPERIMENTAL INVESTIGATION	7
2.1 General	7
2.2 Design of The Folded Plate Model	7
2.3 Construction of The Model	10
2.4 Instrumentation	14
2.5 Loading System	15
2.6 Testing- Safety Measures	16
CHAPTER III: BEHAVIOUR OF THE FOLDED PLATE MODEL	20
3.1 General	20
3.2 Load Vs Strain	20
3.2.1 Longitudinal	20
3.2.2 Lateral	21
3.2.3 Rosettes-Observation	22

3.3	Load Vs Deflection	22
3.4	Load Vs Crack-propagation	23
CHAPTER IV: THEORETICAL INVESTIGATION		25
4.1	Ultimate load of the Folded- Plate Model as a Beam and its Comparison with the Experimentally Observed Ultimate- load.	25
CHAPTER V : CYLINDRICAL SHELL DESIGN- A NEW METHOD		29
5.1	Proposition of a New Method of Design of Reinforcement in Cylindrical Shell Structures.	29
CHAPTER VI: CONCLUSIONS AND RECOMMENDATIONS		44

LIST OF FIGURES

- Figure 1 : Isometric View Of Folded Plate Model with Dimensions.
- Figure 2 : Isometric View of Interior Form Work of Model with quarter-inch groove for shrinkage of wood.
- Figure 3 : Reinforcement in Outer Slant Fold and Top Horizontal Fold.
- Figure 4 : Reinforcement in the Middle Fold and Inner Slant Fold.
- Figure 5 : Reinforcement in the Middle-Fold with SA-4 Strain Gauges.
- Figure 6 : Reinforcement in the Diaphragm
- Figure 7 : Reinforcement in the Model, Full View
- Figure 8 : Location of Strain- Gauges on the Model
- Figure 9 : Location of Dial- Gauges on the Model
- Figure 10: Six layers of Sand Bags; Working Load
- Figure 11: Strut-supports to prevent toppling of sixteen layers of Sand-bags.
- Figure 12: Two layers Sample Loading with dial-gauges positioned on the floor.
- Figure 13: Cracks in West-side Edge-Beam and adjacent Slant Fold, also one channel and one angle iron laid as safety-measure.
- Figure 14: Cracks in East-side Edge Beams, Exterior Surface
- Figure 15: Load Vs Longitudinal Strain
- Figure 16: Load Vs Lateral Strain
- Figure 17: Load Vs Vertical Deflection at mid Span
- Figure 18: Load Vs Vertical Deflection at quarter Span

- Figure 19 : Load vs Horizontal deflection of edge beams.
- Figure 20 : Cracks in West-side Slant Fold, Interior Surface
- Figure 21 : Cracks in West-side Slant Fold Interior Surface
- Figure 22 : Cracks in Middle Fold Interior Surface
- Figure 23 : Reinforcement at Mid-span Section
- Figure 24 : Strain diagram and Stress-diagram
- Figure 25 : Stress-Discontinuity Lines over Cylindrical Shell Model in plan
- Figure 26 : Uniformly distributed Load 'P' and angle ' θ '
- Figure 27 : Dial-gauges' cylindrical supports
- Figure 28 : Cross-section, Strain-diagram Stress-diagram and force diagram.

DEFINITIONS

r	Radius of the Cylindrical Shell or Plate
s	Stress in Steel Reinforcement
t	Thickness of the Cross-section at top
A_c	Total Compressive Area in Concrete
d	Distance of the bottom most Reinforcement from top
E_c	Modulus of Elasticity of Concrete
E_s	Modulus of Elasticity of Steel
f'_c	Concrete cylinder strength
f_c	Maximum compressive stress in concrete from proposed curve
f_s	Stress in Steel
f_{ult}	Ultimate Stress in Steel
k_1	Average Stress in Concrete/Maximum Stress in Concrete
k_2	Depth of Compressive resultant/ Depth of neutral axis
k_3	Maximum stress in Concrete/Cylinder Compressive Strength
l	Transverse Span of folded Plate or Cylindrical shell
L	Longitudinal Span
n	Modular Ratio of Steel and Concrete
M_x	Moment in x-direction
M_{xt}	Twisting Moment
M_u	Ultimate Moment
M_ϕ	Moment in ϕ - direction
n	Depth of Neutral Axis from Top
N_x	Membrane Force in x-direction
$N_{x\phi}$	Shear-force in x-direction on ϕ - plane

u_ϕ	Membrane force in ϕ - direction
u_x	Component of internal load in x - direction
u_y	Component of internal load in y - direction
u_z	Component of internal load in z - direction(normal to the Surface)
u_x	Shear-force on x plane
u_ϕ	Shear-force on ϕ - plane
T_s	Total Tensile force in Tensile Reinforcement
α	Load Dispersion Coefficient in x - direction, Region I
β	Load Dispersion Coefficient in x - direction, Region II
ϵ	Strain
ϵ_c	Strain in Concrete
ϵ_{cu}	Ultimate Strain of Concrete
ϵ_o	Strain Corresponding to f_o'' in Proposed Curve
ϵ_{sy}	Yield Strain of Steel
ϵ_{ult}	Ultimate Strain in Steel
σ_c	Stress in Concrete
σ_{cu}	Concrete Cube Strength
σ_y	Yield Stress of Steel
θ	Angle subtended at the Centre of Curvature by an arc of Cyl. Shell.
θ_o	Semi-angle subtended by cylindrical shell surface at the Centre of Curvature.

C H A P T E R I
I N T R O D U C T I O N

1.1 A brief history of the evolution of the art of analysis and design of the folded plate structures.

The construction of the folded plate structures started in twenties. The theories came later, the first rigorous theory being given by Gruber^{(1)*} in 1937. Later Canfor⁽²⁾, Simpson⁽³⁾, Whitney⁽⁴⁾ and others brought up their simplified theories. Canfor and Simpson took the basic structure as a folded plate with rigid-joints. The joint-displacements were superimposed later. Whitney took the basic structure as a folded plate with hinged-joints and later superimposed the effects of the moments.

Current methods of analysis and design of the folded-plate structures are the following:

- (a) Beam method
- (b) Folded plate theory neglecting joint displacement
- (c) Folded plate theory considering joint-displacement
- (d) Elasticity method

In beam method, the cross-section is analysed and/ or designed as a simple beam. For design, the shape of the cross-section has to be assumed as the method does not give any basis for the choice of the same. Also, at any cross-section, the shear-stress variation along the width of the individual folds

* The number in square bracket shows the reference number listed in the reference list.

is not given. But the method has its simplicity in the application at any limit state of stress i.e. elastic, yield or ultimate, of course, with the necessary assumptions. The model tests conducted by different authors reveal that this method underestimates the collapse load of folded plate structures.

In Methods (b) and (c), i.e. The Folded Plate Theory, each fold of the structure is analysed and designed separately. In the transverse direction, the fold is designed in strips for the normal component of the load as a continuous beam on any yielding supports. This is called the slab-action. Next the fold is considered as a deep beam and longitudinal reinforcement is assigned for the in-plane component of the load. This is called the beam action. The inplane component is due to: one, the resolved part of the external load, and second, the resolved part of the reactions at the edges from the slab-action.

In the beam action, the top and bottom edges of each fold deflect in their own planes and thus incompatibility at each ridge or valley line is created. If the folded plate is heavily reinforced and is strong in transverse direction, the incompatibility is not severe and is neglected. This is method(b). If the incompatibility is not negligible, then relative joint - displacements are calculated and the continuity- conditions are applied. This is method(c).

In methods(b) and (c), after the elastic analysis of the structure, the reinforcement can be designed in accordance with ultimate strength theories. But this design will be quite different from the beam method, because, in this method, all the

valley-lines irrespective of their level, will be assumed to be at the ultimate strain stage of steel whereas according to beam method, the same valley-lines will be at different strains, the strain being linearly proportional to the distance from the neutral axis.

The fourth and the most accurate method termed as the Elasticity Method is after Goldberg and Levy⁽⁵⁾. The folded plate is analysed under combined membrane and plate-bending actions. Transverse edge is assumed to be simply supported.

The joint-displacements are expanded in terms of half-range Fourier-series. The joint-forces are taken as the combination of joint-displacements, in a manner similar to the slope-deflection equations for a unidimensional member.

Using a semi-inverse approach, the problem is solved to yield, at every point of the plate, the bending moment, twisting moment, direct force and shearing force in longitudinal as well as lateral direction. The method is enhanced due to the fact that a computer-analysis is provided by Goldberg, Glauz and Setlar⁽⁶⁾.

In the first three methods, the analysis as well as design were discussed simultaneously. The fourth method, besides being most accurate, is more cumbersome than the first three if a hand computation is contemplated. The simplicity of its analysis was overcome with the advent of computer, but that of the design remained to be a challenge. If not impossible, it became most difficult to place the reinforcement along the principal stress trajectories obtained from the stress results of the elasticity method of analysis.

A more practical approach would be to place as far as possible an orthogonal set of reinforcement except in the zones where the principal stresses make an angle close to 45° to the coordinate direction. A brief account of a design procedure incorporating the above idea is explained in Article 2.2 of Chapter II.

1.2 Aim Of The Present Study

The present study comprises of the following three items :

1.2.1 Experimental Verification Of The Proposed Method Of Design Of Folded Plate Structures.

1.2.2 Comparison Of The Experimental Results With The Existing Ultimate Strength Theories Of The Folded Plate Structures.

A reinforced concrete folded plate model(10'x7' in plan) was tested in the laboratory. The strains and deflections at different stages of loading were observed and compared with the theoretically obtained values. The behaviour of the model is described in Chapter III. The ultimate load of the test was compared with the ultimate load obtained by the simple beam method. The details of the comparison are given in Chapter IV.

1.2.3 Proposition Of A New Approach For The Design Of Folded Plate Structures And Cylindrical Shells

Complete analysis of the folded plate structures or cylindrical shells is a cumbersome problem. The solution of five or more equilibrium equations takes time. After all the unknown parameters are evaluated, the reinforcement is designed. Although, with the advent of computer, the problem can be solved more readily, computers are available to everyone. Therefore, the need of an easier method of analysis and/or design arises. Billington (7-8) has given two methods of the design of

simply-supported slabs. In the first method of design, the modified moments M_x^* and M_y^* are obtained by adding the twisting moments to the moments in x and y directions as follows:

$$M_x^* = M_x \pm |M_{xy}|$$

$$\text{and } M_y^* = M_y \pm |M_{xy}|$$

M_x^* and M_y^* are formed as the design moments. Plus or minus sign is used depending upon the direction of M_{xy} . Wood⁽⁹⁾ has elaborated the same method in greater detail.

The second method is known as the Hillerborg's strip method⁽⁸⁾, whereas the first method needs the complete analysis before it can be applied to design, the strip method is a direct method of design. The design moments are directly obtained from the uncoupled equilibrium equations. The Hillerborg's strip method is derived from the Equilibrium Theory⁽¹⁰⁾.

Unfortunately, both these methods are restricted to the slabs under the pure moment field.

The folded plates and the cylindrical shells are subjected to the moments as well as the direct forces. The problem of the folded plate structures and its solution, both are discussed in the last para of the Article 1.1 of the Chapter 1.

When a cylindrical shell surface under load meets the boundaries, the axial and the bending forces are generated. For the analysis of the cylindrical shells, different investigators have proposed different bending theories. Out of all these theories, the Donnell-Karman-Jenkins (abbreviated as D-K-J) Theory⁽¹¹⁾ is the most accurate one. After this accurate analysis, design and fabrication of the reinforcement still remain the problems

as the reinforcing bars need to be laid along arbitrary space curves.

To solve the above problems, a method has been evolved in the Chapter V. Hillerborg's strip method has been extended and applied to find the axial force and the bending-moment at any point on the cylindrical shell surface. The reinforcement is then, designed by the ultimate strength theory at every point in two orthogonal directions. This is specifically a design procedure. The five equilibrium equations in terms of eight unknowns N_x , N_ϕ , $M_{x\phi}$, M_x , M_ϕ , $N_{x\phi}$, Q_x and Q_ϕ of D-K-J theory are reduced into two equations with four unknowns N_x , N_ϕ , M_x and M_ϕ . In the process $M_{x\phi}$ is neglected and Q_x , Q_y and $N_{x\phi}$ are eliminated. Each of these two equations, is uncoupled into two sub-equations with the help of a load-dispersion coefficient whose value is known in different regions on the surface of the cylindrical shell. These four sub-equations are then easily solved for N_x , N_ϕ , M_x and M_ϕ which are the required design-forces and design-moments to calculate the reinforcement.

CHAPTER II

EXPERIMENTAL INVESTIGATION

2.1 General

Through tests, we always try to see the overall structural behaviour of a structure. Concrete is an unpredictable material. Folded plate behaviour is non-linear one. Cracking and redistribution of stresses make it still more intricate. All this signifies the need of the actual tests to understand the structural behaviour of folded plates at all stages of loading.

A reinforced concrete model of a simple span folded plate was constructed and loaded to collapse. The load was applied by means of sand-bags. Cracking of the model was carefully observed and marked sequentially. Deflections and strains were measured after each step of loading.

2.2 Design Of The Folded Plate Model

For design of the model the method proposed by Suryanarayana⁽¹²⁾ was used. By the elasticity method⁽⁵⁾ of analysis of folded plate structures, M_x , M_y , M_{xy} , N_x , N_y and N_{xy} were obtained. The remaining procedure, due to Suryanarayana⁽¹²⁾ is as follows:

- (a) Calculate bending stresses σ_{bx} , σ_{by} , σ_{bxy} from M_x , M_y , M_{xy} resp. (sagging moment-positive).
- (b) Calculate membrane stresses σ_{mx} , σ_{my} , σ_{mxy} from N_x , N_y , N_{xy} resp. (tensile membrane force-positive).
- (c) Calculate the combined stresses at three levels of the depth of section:

At top $\sigma_x(1) = \sigma_{bx} - \sigma_{nx}$, $\sigma_y(1) = \sigma_{by} - \sigma_{ny}$, $\tau_{xy}(1) = \sigma_{bxy} - \sigma_{nxy}$

At middle $\sigma_x(2) = \sigma_{nx}$, $\sigma_y(2) = \sigma_{ny}$, $\tau_{xy}(2) = \sigma_{nxy}$

At bottom $\sigma_x(3) = \sigma_{bx} + \sigma_{nx}$, $\sigma_y(3) = \sigma_{by} + \sigma_{ny}$, $\tau_{xy}(3) = \sigma_{bxy} + \sigma_{nxy}$

- (d) Calculate the principal stresses and their directions at top, middle and bottom, (J=1,2,3):

$$\sigma_1(J) = \frac{\sigma_x(J) + \sigma_y(J)}{2} + \left[\frac{\{\sigma_x(J) - \sigma_y(J)\}^2}{4} + \tau_{xy}^2(J) \right]^{1/2}$$

$$\sigma_2(J) = \frac{\sigma_x(J) + \sigma_y(J)}{2} - \left[\frac{\{\sigma_x(J) - \sigma_y(J)\}^2}{4} + \tau_{xy}^2(J) \right]^{1/2}$$

$$\text{and } \theta(J) = \tan^{-1} \frac{2\tau_{xy}(J)}{\sigma_x(J) - \sigma_y(J)}$$

- (e) Check: If Absolute ($\sigma_x - \sigma_y$) < 0.01, assume

$$\theta = 45^\circ,$$

- (f) Check: If $\sigma_1(J) > \sigma_c$ or $\sigma_2(J) > \sigma_c$, (J=1,2,3) ,
Thickness is too small.

- (g) If $\theta = 45^\circ$, the reinforcement is calculated as below:

Top layer major principal stress direction

$$A_{st1} = \frac{\sigma_1(1) + \sigma_1(2)}{f_s}$$

Top layer minor principal stress direction

$$A_{st2} = \frac{\sigma_2(1) + \sigma_2(2)}{f_s}$$

Bottom layer major principal stress direction

$$A_{sb\ 1} = \frac{\sigma_1(2) + \sigma_1(3)}{f_s}$$

Bottom layer minor principal stress direction

$$A_{sb\ 2} = \frac{\sigma_2(2) + \sigma_2(3)}{f_s}$$

- (h) If $\theta \neq 45^\circ$, the modified stresses hereafter called the design stresses are first calculated for top, middle and bottom as below; ($J=1,2,3$):

$$\sigma_x^*(J) = \sigma_x(J) + \text{Absolute} (\tau_{xy}(J))$$

$$\sigma_y^*(J) = \sigma_y(J) + \text{Absolute} (\tau_{xy}(J))$$

- (i) If $\sigma_x^*(J)$ is negative, assume

$$\sigma_x^*(J) = 0$$

$$\sigma_y^*(J) = \sigma_y(J) + \text{Absolute} (\tau_{xy}^2(J) / \sigma_x^*(J))$$

If the later value of $\sigma_y^*(J)$ is negative, assume

$$\sigma_y^*(J) = 0$$

- (ii) If $\sigma_y^*(J)$ is negative, assume

$$\sigma_y^*(J) = 0$$

$$\sigma_x^*(J) = \sigma_x(J) + \text{Absolute} (\tau_{xy}^2(J) / \sigma_y^*(J))$$

If the later value of $\sigma_x^*(J)$ is negative, assume

$$\sigma_x^*(J) = 0$$

(iii) The reinforcement in x and y directions is calculated as below:

Top layer, x - direction

$$A_{sta} = \text{Absolute} (\sigma_x^s(1) + \sigma_x^s(2)) \text{ divided by } f_s$$

Top layer, y - direction

$$A_{sty} = \text{Absolute} (\sigma_y^s(1) + \sigma_y^s(2)) \text{ divided by } f_s$$

Bottom layer, x - direction

$$A_{sbx} = \text{Absolute} (\sigma_x^b(2) + \sigma_x^b(3)) \text{ divided by } f_s$$

Bottom layer, y - direction

$$A_{sby} = \text{Absolute} (\sigma_y^b(2) + \sigma_y^b(3)) \text{ divided by } f_s$$

2.3 Construction Of The Model

(a) Form-work

The configuration and dimensions of the model are shown in Figure(1). The inner form work was constructed from 1" thick wooden planks. For edge beams and end-diaphragms back form work was constructed. The slant folds inclined at 45° from vertical did not need any back form work. The back form work was such that it could be unscrewed very easily just after three days of concreting. Special care was taken in the construction of form work. So that it could be removed from the concrete without ruining it. For longitudinal and lateral shrinkages of the wood quarter-inch wide grooves were provided as shown in Figure(2).

(b) Reinforcement

The reinforcement was installed in three phases:

- (1) Transverse steel (bottom layer, clear cover $1/8"$)

(ii) Longitudinal Steel(middle layer)

(iii) Transverse steel(top layer, clear cover 1/8")

For reinforcement, local steel bars in two sizes viz. 1/8" diameter(exact diameter 0.126") and 1/4" diameter(exact diameter 0.236") were used. The 1/4" diameter steel was needed for middle-fold longitudinal reinforcement. For the rest of the steel reinforcement 1/8" diameter steel was used. Longitudinal reinforcement near end diaphragms was to be kept at 45° as required in design in one foot length from either diaphragm. The longitudinal steel was then extended for end-diaphragm reinforcement. Spacing of lateral reinforcement for different folds was calculated such that the bars from one fold could be continued to the adjacent folds. This reduced the number of bars required to a minimum.

The lengths of such bars were measured from the drawing and were cut out to exact sizes. Curved bars were straightened and bent to the required form. For installing the reinforcement at the required depths, small steel cylinders were used in between two layers of reinforcement. Reinforcement-details are shown in figure(3,4,5,6 and 7).

Properties of reinforcement Steel:

Diameter	Yield Stress	Ultimate Stress	Ultimate Strain
0.236"	82000 psi	82250 psi	0.0250
0.126"	81000 psi	83000 psi	0.0204

These properties were determined through the actual test in laboratory in Sinus-Olsen Testing Machine on 3" long test-pieces. Three test-specimen were used for each diameter.

After the complete installation of reinforcement, back-form work for end-diaphragms and edge beams was fixed by means of 3/16" screws.

Two 2" brick walls of length 3 feet and height 3 feet were constructed at 10'-2" c/c distance. After three days of curing, the form work with reinforcement was mounted over the brick-walls for concreting.

Six MI-4 strain gauges were fixed to the 1/4" diameter longitudinal steel for strain measurement as shown in Figure(5).

(c) Concreting

Mix-Design:

Mix proportion by weight = 1½:2:4

Water-cement ratio = 0.7

Materials used per batch,

Portland cement* = 35 Kg.

Sand = 56 Kg.

3/8" Size Aggregate = 112 Kg.

Out of 56 Kg of sand, fine sand was 42 Kg. and coarse sand was 14 Kg.

Item	Specific Gravity	Fineness Modulus
Fine Sand	2.65	1.79
Coarse Sand	2.65	2.99
Aggregate	2.65	-

* Due to poor gradation of sand and aggregate, 7 Kg more cement was added to the original quantity of 28 Kg.

Concreting was done in three batches. To preserve the reinforcement from dislocation, curing of concrete needed utmost care.

For quality control, two cubes from each batch were casted. The thickness of concrete had to be one inch except that of the edgebeams and end-diaphragms, therefore vibrator could not be used for compaction in the solids.

Total concreting took five hours. The work was conducted in the evening from 5 P.M. to 10 P.M.

(d) Curing

Curing was started after 16 hours. Whole of the exposed surface was covered by gunny bags after dipping them in water. Later water was sprayed over them four-times daily. The test-cubes were cured by keeping them submerged under water. Curing was stopped after twenty four days for carrying out the instrumentation work.

(e) Removal of form work

On third day, back form work of edgebeams and end-diaphragms was removed. Interior form-work was removed on seventh day. For removing the form work of diaphragms, the model had to be lifted above its supporting-walls. In the process, a short diagonal crack developed in the edge beam at north-east corner. Longitudinal honey-combing in outer slant folds near ridges was also observed when interior form work was removed. Both of these were suspected as weak-spots on the model but through testing they were found to be all-right.

3.4 Instrumentation

(a) Strain Measurement

Figure(3) shows the location of all the strain gauges used. Table No. 1 gives the details of the gauges.

Table No. 1

S.No. of Channel	Type of Gauge	Gauge factor	Nominal Gauge length
1 to 6	SR-4 A-5-BG	1.98	-
7 to 12	Rosettes SAR-5R	2.02	5 mm
13 to 15	ET - 10	1.98	10 mm
16 to 38	CT- 12	2.01	12 mm

For thirty-eight strain gauge channels, two switching units with one strain-indicator and three switching and balancing units with another strain-indicator were used. Channels from serial number 1 to 10 were connected to first switching unit and from serial number 11 to 15 to the second switching unit. Both of these units were then connected to a strain-indicator. Channels from serial-number 16 to 25 were connected to the first switching and balancing unit, serial number 26 to 35 to the second switching and balancing unit and from serial number 36 to 38 to the third switching and balancing unit. All these three were then connected to a second strain-indicator. For temperature compensation, dummy strain-gauges one SR-4 strain-gauge for channels 1 to 6 on the steel and one rosette SAR-5R for channels 7 to 12, one ET-10 strain-gauge for channels 13 to 15 and one CT-12 strain-gauge for channels 16 to 38 all on concrete were

used.

Half bridge circuit was used for strain measurements, there being two active gauges, one on the model and another dummy gauge on steel-bar-piece or the concrete cube.

(b) Deflection Measurements

Figure(9) shows the location of all the dial-gauges.

Total thirty dial-gauges were used, twenty-four for measuring vertical deflections and six for measuring horizontal deflections.

For installing the dial-gauges, thirty concrete cylindrical supports were casted with 8" long slotted angle-irons embedded in them. To this embedded slotted angle, another piece of slotted angle of required height was connected by means of screws, at the top of which the dial-gauges was fixed to read the deflection of the desired point on the model. Thus after all the thirty dial-gauges were positioned, the supports were rigidly fixed to the floor with the help of plaster of paris.

(c) Special Details

Whole of the interior and exterior surface was white-washed for easy observation of cracks.

To avoid any unexpected crushing of brick-walls beneath the end-diaphragms under heavy loading, two, eight feet long, four inches wide and quarter-inch thick steel bearing plates were used.

2.5 Loading System

As the loading on the inclined folds poses practical problems, only the horizontal folds were loaded in the experiment and the folded plate was analysed and designed for this loading case. In uniform loading over the whole surface of the folded plate,

the load contribution from the outer slant fold 2-3 (Refer Figure 1), was kept on the adjacent horizontal fold 3-4. Similarly the load of folds 4-5 and 6-7 was kept on middle horizontal fold 5-6. Thus the load on fold 5-6 was 1.51 times the load on the fold 3-4 or fold 7-8.

The folded plate model had been designed for a load of 333 psf on middle horizontal fold and a load of 221 psf on the other two horizontal folds. This was equivalent to 100 psf of average load on whole surface.

For loading, sand-bags and bricks were the two choices. With bricks, there seemed greater possibility of arch action with the increasing central deflection. Besides, piling bricks on horizontal folds would have needed more head-room for the same load compared to sand bags. Therefore sand bags were used as a better choice. The bags were kept one above the other and it was seen that the columns of sand bags did not have any interaction with each other. This assured that the loading was directly transferred to the folded plate uniformly and there was no arch-action.

2.6 (a) Testing

All the instrumentation was checked thoroughly before the test was started. The test-programme was proposed to be executed in two phases:

- (I) To load the model upto working load and then to unload it, Figure(10).
- (II) To load the model upto collapse load, Figure(11).

The purpose of the first phase was to get acquainted with the practical difficulties in loading sand-bags and reading strain-gauges and strains. The testing was done in steps. Each

step consisted of the following:

- (a) To place 6, 66 lb. bags on middle horizontal fold.
- (b) To place 6, 33 lb. bags on one upper horizontal fold.
- (c) To place 6, 33 lb. bags on other upper horizontal fold.
- (d) To place 6, 66 lb. bags on middle horizontal fold.
- (e) To read the dial gauges.
- (f) To read the strains.

A two layer sample loading(two steps) with the dial-gauges positioned on floor is shown in figure(13).

Average intensity of loading obtained per step was 21.34 psf. The model was loaded upto fourth step i.e. 85.36 psf. No. cracks were visible on the structure. Loading was then removed.

Second phase of loading was started next-morning. Zero-load readings were taken, loading was then started. Upto five steps of loading i.e. 106.7 psf average, there was no sign of crack.

The first-cracks were observed through sixth step of loading i.e. 128 psf average. They were immediately marked. Through eighth step of loading i.e. 171 psf average, the middle half span had developed the cracks roughly at every one foot interval of edge-beams and middle horizontal fold. The cracks, due to longitudinal bending tensile stress, had propagated transversely from bottom fibre upto approximately the half-depth of slant-folds.

The sand-bags were substituted as the test was stopped for three days. One hundred bags were again prepared. It was expected that the model will collapse within twelve steps of

loading 2.0. 500 psi average. But the structure was still quite intact. All previous cracks had propagated further. New cracks appeared only in the middle fold in outer quarter-spans but not in edge-beams. No longitudinal crack was so far observed. One hundred bags were again prepared and the model was loaded. This was after one week of previous loading. Through fifteenth stop of loading, the model had shown enormous cracks, Figure (11). Complete collapse was expected in sixteenth stop, therefore, all instrumentation was removed. Sixteenth layer of bags was kept very carefully. Against everybody's expectation the model still stood. Long diagonal cracks in the inner slant folds had propagated from the lower edge upto the upper edge at 45° approximately.

By this time, the height of bags laid over the model was nearly twelve feet. Bags were all exhausted. Further laying of bags had become very difficult and risky. The head-room, also, was not available, Figure(11). Therefore, the test was abandoned here.

(b) Safety-Measures

For reading dial-gauges, at every step of loading, a man had to go beneath the model. For his safety, two channels, one at mid-span and other at quarter span were laid just two-inches below the edge beams, in the transverse direction, Figures(13,14) so that if the model collapses suddenly, it will rest on the channels and not reach to the floor.

After twelve layers of bags on the model, the height of bags was nearly ten feet. The area on which these bags rested was only one foot wide, so that bags were much expected to topple in transverse direction. The labourers had to walk over the bags for laying new bags. Therefore to prevent the toppling, side-struts

were fixed, as shown in Figure(11). Small wooden struts were also fixed between the middle pile and side piles, so that the side piles may not fall towards middle one. For the safety of labourers, walking at the top of barge, a rope was hung from the roof truss as shown in Figure(11).

Behaviour of the model is explained in Chapter III.

CHAPTER III

BEHAVIOUR OF THE FOLDED PLATE MODEL

3.1 General

The behaviour of the model has been described in three periods of loading. Strain-variation, deflection and crack-propagation are discussed for each period of loading. The time-effects of the sustained loading between two consecutive loading-periods are also discussed. Henceforth, this effect would be termed as the time-effect in between two periods of loading. The strain-readings are not fully reliable, however, the best possible usage has been made of their variation, in bringing-out the facts of actual behaviour of the model and of the redistribution of stresses in the lateral and longitudinal directions.

3.2 Load Vs Strain

For the location of the strain-gauges see Figure (8).

3.2.1 Longitudinal(Refer Figure(15))

The total longitudinal strain-behaviour observed through fourteen strain-gauges can be summed up as follows:

Throughout the first period of loading(upto 170 pounds per square foot average) the whole mid-span cross-section showed the tension including the upper horizontal folds. The time-effects of the sustained loading was that the middle fold showed further tension, whereas the edge beams' strains reduced.

Throughout the second period of loading(upto 356 psf. average) again the whole mid-span transverse section showed tension. The time-effect of the sustained loading was just reverse of the earlier time-effect. The strains in the middle fold were very much reduced whereas the strains in edge-beams

increased by an increment greater than their original values.

Through the third and final period of loading(upto 341 psf average), the whole mid-span cross-section underwent elongation .

According to the magnitude, the tensile strains were higher in the middle-fold compared to the edge-beams, although the bottom fibre of the middle fold was four-inches above the bottom fibre of the edge beam where the longitudinal strains were measured. Through the first time-effect and the second period of loading, the middle fold elongated more compare to the edge-beams. The second time-effect changed the whole pattern of the strains. whereas the strains in the middlefold came down to very small values, the strains in the edge-beams increased to very high values.

3.2 Lateral(Refer Figure(16))

The total lateral strain behaviour observed through the eighteen strain-gauges(Figure(8)) can be summed up as follows:

The lateral strains have shown the constant increase with the increase in the load.

Throughout the first period of loading(upto 170 psf average) the strains increased non-linearly with the load. The time-effect of the sustained loading reduced all the tensile strains and increased all the compressive strains. The original tensile strains on mid-span of the middle fold increased by a small increment .

Throughout the second period of loading(upto 256 psf average) the strains again increased non linearly with the load. The time-effect of this sustained loading was to increase all the tensile strains by an increment greater than their original values. Even the compressive strains at the upper edge of the slant ends showed the large tension strains. Exceptions were the two straight-

gauges fixed in the middle fold at mid-span whose original large tensile values were changed to the compressive values.

Throughout the third period of loading(upto 341 psf average) the strains again increased with the loading.

The mid-span strain-gauge readings reflect that the prototype behaviour on either sides of the longitudinal centre line was not identical.

3.2.3 Rosettes Observation

Through the first period of loading, the rosettes, figure(8), showed constantly increasing tensile strains. The time effect of the first sustained loading(170 psf. average) was to boost up the original values by the increments greater than the original values.

Through the second period of loading, again the strains were increasing. The time-effect of this sustained loading(286 psf. average) was just reverse of the earlier time-effect. All the strains changed to the compressive values.

Through the third period of loading,(upto 341 psf. average) the compressive strains kept reducing.

3.3 Load Vs Deflection

Dial-gauge locations are shown in Figure (9).

The observed vertical deflections are more as we move from the edges towards the centre. The maximum vertical deflection of 9.97 mm was observed at mid-span of the middle fold which was more than double the deflection of mid-span points on the edge-beams.

One typical observation was that, whereas the west-side edge beam showed more deflection compared to the east-side edge

beam, the west-side upper horizontal fold showed less deflection compared to the east-side upper horizontal fold.

The load-deflection graphs are shown in figures(17,18,19). The graphs show a non-linear variation upto the final observations. As the curves do not show any yield in deflections, it is supposed that the structure would have taken still more load.

The horizontal deflections measured at quarter, half and three-quarter spans of edge beams on the exterior sides do not seem to be reliable as their variation is too random, figure(19).

3.4 Load Vs. Crack-propagation

Cracks were observed on the whole interior surface and on the exterior surface of edge beams and the adjacent slant-folds.

The first transverse crack was observed at 123 psf.(average) of load in the east edge-beam at mid-span. In the next step of loading i.e. at 140 psf.(average), the other edge-beam cracked at mid-span and quarter span. The first crack of the west edge-beam propagated further with no crack at other sections.

The first transverse crack in the middle fold was observed at 170 psf.(average) at mid-span and quarter span. At this loading, the east edge-beam also cracked at the quarter span. Through the next step of loading i.e. 190 psf.(average), cracks were observed at three quarter span in both edge beams as well as in the middle fold. The middle-fold cracked at two more sections between the mid-span and three quarter span. The cracks of the edge beams propagated through their full depth of 4" in the adjacent folds, through approximately half of their slant-depths.

Thus at every step of loading, the old cracks propagated further and the new cracks developed.

At 256 psf. (average) of loading, the middle half span had developed the cracks at an approximate spacing of one foot.

Through the third period of loading, the edge beams did not show any new cracks. The old cracks propagated through the adjacent slant folds upto nearly two-inches from top-edges at mid-span and upto four-inches from top edges at other sections. The middle fold showed new cracks in the remaining span-lengths also. The nearest cracks were one-inch from the end diaphragms. In fifteenth and sixteenth steps of loading i.e. 341 psf.(average), the inner slant folds cracked diagonally. The diagonal cracks started from the edge of the middle-fold from a point about one-foot away from the end-diaphragm, at 45° in the slant fold and reached upto its top edge.

In the whole structure, only a single small longitudinal crack was observed in the middle fold in the last quarter span.

When all the loading was removed after ten days, similar diagonal cracks were observed in the inner slant folds at the top surface. These diagonal cracks had propagated longitudinally along the upper edges of the slant folds to join each other.

The upper horizontal folds did not show any cracks at all.

The cracks in different folds are shown in Figures (13,14, 20,21 and 22).

CHAPTER IV

THEORETICAL INVESTIGATION

4.1 Ultimate Load Of The Folded Plate Model As A Beam:

In the following lines, the ultimate load of the folded - plate has been calculated from its ultimate moment capacity at the mid-span section. The reinforcement is shown in Figure(22). The twenty-two bars in slant folds are distributed in seven layers. They have been assumed to be placed at one point in the middle of those seven layers. This assumption does not cause any error because the bars are identically placed above and below that level. Thus the total bars in the section are now assumed to be in seven layers instead of thirteen layers.

Usual assumptions of simple bending theory are made in this calculation also. For calculating the compressive stress at top in concrete, Hognested stress-strain curve has been used.

Neutral axis is assumed to be at 2" from top(Different values were tried but 1" depth gave best comparison of compressive and tensile forces).

Example: Refer Figure(23 and 24)

Data:

Concrete cube strength : σ_{cu} = 4000 psi

Material properties of reinforcing steel:

	Yield		Ultimate	
	1/8" dia. bars	1/4" dia bars	1/8" dia bars	1/4" dia bars
Stress	81,000 psi	82,000 psi	88,000psi	82,800 psi
Strain	0.0145	0.0167	0.0204	0.0250

Using suggested stress-strain curve for concrete:

$$E_c = 18,000,000 + 400 \times f_c''$$

$$f_c'' = 0.85 f_c'$$

$$f_c' = 0.80 \sigma_{cu}$$

$$\epsilon_c = 2 f_c'' / E_c$$

$$f_c = f_c'' \left[2 \frac{\epsilon}{\epsilon_c} - \left(\frac{\epsilon}{\epsilon_c} \right)^2 \right]$$

Strain in the top fibre of concrete in compression(from strain diagram, Figure(24))

$$\epsilon = \frac{\epsilon_{max}}{d-n}$$

$$= \frac{0.0204}{16-1}$$

$$= \frac{0.0204}{15}$$

$$= 0.00136$$

$$f_c' = 0.80 \times 4900 = 3920 \text{ psi}$$

$$f_c'' = 0.85 \times 3920 = 3330 \text{ psi}$$

$$E_c = 1800,000 + 400 \times 3330 = 3330,000 \text{ psi}$$

$$\epsilon_c = 2 \times 3330 / 3330,000 = 0.002$$

$$f_c = 3330 \left[2 \times \frac{0.00136}{0.002} - \left(\frac{0.00136}{0.002} \right)^2 \right]$$

$$= 3330 (1.36 - 0.46)$$

$$= 300 \times 0.90$$

$$= 2997 \text{ psi}$$

Compressive force in concrete above the neutral axis:

$$C_u = 2/3 \times f'_c \times 0.85 \times n \times b$$

$$= 2/3 \times 2997 \times 0.85 \times 1 \times 24$$

$$= 40800 \text{ lbs.}$$

(For calculation of C_u , above formula holds because for 1" from top, the section is composed of two horizontal folds. For the depth more than 1" , the formula will not hold)

Tensile force in steel bars below the neutral axis: (Refer Figure(24))

$$\begin{aligned} T_u &= 49000 \times 0.0496 + 71000 \times 0.2728 \\ &+ 51000 \times 0.172 + 81000 \times 0.0248 \\ &+ 4 \times 80000 \times 0.0248 \\ &= 9455 + 19400 + 8770 + 2010 + 8240 \\ &= 40375 \text{ lbs.} \end{aligned}$$

Taking moment about neutral axis

$$\begin{aligned} M_u &= 2485 \times 4.85 + 19,400 \times 7.8 \\ &+ (8700 + 2000) \times 10.9 \\ &+ 8000 \times (13 + 13.7 + 14.5 + 15.1) \\ &+ 41000 \times (1 - 0.5 \times 0.85 \times 1) \\ &= 10,400 + 151,000 + 117,000 + 116,000 \\ &\quad + 87,000 \\ &= 482,000 \text{ lb-inches} \\ &= 39300 \text{ lb-ft} \end{aligned}$$

$$\begin{aligned}
 M_{fl_{max}} &= P_u \times \frac{L}{8} \\
 &= P_u \times \frac{10}{8} \\
 &= 1.25 P_u
 \end{aligned}$$

Equating the external Bending Moment to ultimate moment capacity of the section

$$\begin{aligned}
 P_u &= \frac{35300}{1.25} = 28200 \text{ lbs.} \\
 &= 12.57 \text{ tons}
 \end{aligned}$$

Comparison of the Experimental and Theoretical results:

The model under test was loaded to sixteen steps of loading. Each step of loading was equivalent to a total load of 0.825 tons. Thus in the sixteen steps, the total load on the model was 13.2 tons. This is 5% greater than the theoretically obtained load of 12.57 tons. This shows that the model was designed safely, and hence the method adopted in the design of the model can be recommended for the design of the folded plate structures.

CHAPTER V

CYLINDRICAL SHELL DESIGN - A NEW METHOD

5.1 Proposition Of a New Method Of Design Of Reinforcement in Cylindrical Shell Structures:

The analysis and design of cylindrical shell structures involves solution of five equilibrium equations. The unknowns M_x , M_ϕ , $M_{x\phi}$, U_x , U_ϕ and $U_{x\phi}$ are expressed in terms of the displacements u , v and w . Thus the total eleven equations with eleven unknowns are reduced to one eighth-order partial differential equation with one unknown w . The solution of this equation is extremely involved. This arises the need of an easier method for the analysis and/or design of cylindrical shell structures.

Millerborg⁽²⁾ has given a method known as 'strip method' for the design of slabs which is a direct design-procedure. The whole slab surface is divided into regions according to the load-dispersion directions with the help of stress-discontinuity lines, Figure(26). The strips are then designed along load-dispersion directions which is an extremely simple job.

An attempt has been made through this chapter to extend and apply the strip-method in the design of cylindrical shell structures. The original strip method is applied to design the plane slab under the effect of pure moment field. The cylindrical shell surface is a curved surface under the effect of moments as well as membrane forces.

Equations of equilibrium in D.K.F. Theory are as follows:-

$$\frac{\partial M_x}{\partial x} + \frac{\partial M_{x\phi}}{\partial \phi} - P_x = 0 \quad \text{---(1)}$$

$$\frac{\partial H_\phi}{\partial \phi} + a \frac{\partial H_{\phi x}}{\partial x} - Q_\phi - \frac{1}{\phi} a = 0 \quad (1)$$

$$a \frac{\partial H_x}{\partial x} + \frac{\partial H_{\phi x}}{\partial \phi} - a Q_x = 0 \quad (2)$$

$$\frac{\partial H_\phi}{\partial \phi} + a \frac{\partial H_{\phi x}}{\partial x} - a Q_x = 0 \quad (3)$$

$$a \frac{\partial Q_x}{\partial x} + \frac{\partial Q_\phi}{\partial \phi} + H_\phi + \frac{1}{\phi} a = 0 \quad (4)$$

we are five equations in terms of eight unknowns

Differentiating (1) w.r. to x , results in

$$\frac{\partial^2 H_\phi}{\partial x^2} + \frac{1}{a} \frac{\partial^2 H_{\phi x}}{\partial x \partial \phi} + \frac{\partial Q_x}{\partial x} = 0 \quad (5)$$

Differentiating (2) w.r. to ϕ , gives

$$\frac{\partial^2 H_\phi}{\partial \phi^2} + a \frac{\partial^2 H_{\phi x}}{\partial x \partial \phi} - \frac{\partial Q_\phi}{\partial \phi} - a \frac{\partial p_\phi}{\partial \phi} = 0 \quad (6)$$

Dividing (6) by a^2 , gives

$$\frac{\partial^2 H_\phi}{a^2 \partial \phi^2} + \frac{\partial^2 H_{\phi x}}{a^2 \partial x \partial \phi} - \frac{\partial Q_\phi}{a^2 \partial \phi} - \frac{\partial p_\phi}{a \partial \phi} = 0 \quad (7)$$

Subtracting (5) from (7), one obtains

$$\frac{\partial^2 H_\phi}{a^2 \partial \phi^2} + \frac{\partial^2 H_{\phi x}}{\partial x^2} - \frac{\partial Q_\phi}{a^2 \partial \phi} - \frac{\partial p_\phi}{a \partial \phi} - \frac{\partial p_x}{\partial x} = 0 \quad (8)$$

Differentiating (3) w.r. to x

$$a \frac{\partial^2 H_x}{\partial x^2} + \frac{\partial^2 H_{\phi x}}{\partial x \partial \phi} - a \frac{\partial Q_x}{\partial x} = 0 \quad (9)$$

Differentiating (5) w.r. to ϕ

$$\frac{\partial^2 H_\phi}{\partial \phi^2} + a \frac{\partial^2 H_\phi}{\partial x \partial \phi} - a \frac{\partial Q_\phi}{\partial \phi} = 0 \quad \dots(12)$$

Dividing (12) by a

$$\frac{\partial^2 H_\phi}{a \partial \phi^2} + \frac{\partial^2 H_\phi}{\partial x \partial \phi} - \frac{\partial Q_\phi}{\partial \phi} = 0 \quad \dots(13)$$

Adding (12) and (13)

$$a \frac{\partial^2 H_\phi}{\partial x^2} + \frac{\partial^2 H_\phi}{a \partial \phi^2} + 2 \frac{\partial^2 H_\phi}{\partial x \partial \phi} - a \frac{\partial Q_\phi}{\partial x} - \frac{\partial Q_\phi}{\partial \phi} = 0 \quad \dots(14)$$

Adding (5) and (14)

$$a \frac{\partial^2 H_\phi}{\partial x^2} + \frac{\partial^2 H_\phi}{a \partial \phi^2} + 2 \frac{\partial^2 H_\phi}{\partial x \partial \phi} + H_\phi + p_z a = 0 \quad \dots(15)$$

Substituting for $\frac{\partial Q_\phi}{a^2 \partial \phi}$ from (13) in (10)

$$\frac{\partial^2 H_\phi}{a^2 \partial \phi^2} - \frac{\partial^2 H_\phi}{\partial x^2} - \frac{\partial^2 H_\phi}{a^2 \partial x \partial \phi} - \frac{\partial^2 H_\phi}{a^3 \partial \phi^2} - \frac{\partial p_z}{a \partial \phi} - \frac{\partial p_z}{\partial x} = 0 \quad \dots(16)$$

To realize the strip-action, we neglect $H_{xx\phi}$ from equations (15) and (16) as demanded by Millerberg's strip method (7).

Equation (15) thus reduces to

$$\frac{\partial^2 H_\phi}{\partial x^2} + \frac{\partial^2 H_\phi}{a^2 \partial \phi^2} + \frac{H_\phi}{a} + p_z = 0 \quad \dots(17)$$

and equation (16) reduces to

$$a \frac{\partial^2 H_\phi}{\partial x^2} + \frac{\partial^2 H_\phi}{a \partial \phi^2} - \frac{\partial^2 H_\phi}{a^2 \partial x \partial \phi} - \frac{\partial p_z}{\partial \phi} - a \frac{\partial p_z}{\partial x} = 0 \quad \dots(18)$$

Grouping equation (17) into two

$$\frac{\partial^2 H_\phi}{\partial x^2} = -a \left(\frac{\partial^2 H_\phi}{a^2 \partial \phi^2} + \frac{H_\phi}{a} + p_z \right) \quad \dots(17a)$$

$$\text{and } \frac{\partial^2 H_\phi}{a^2 \partial \phi^2} = -(1-\alpha) \left(\frac{H_\phi}{a} + p_z \right) \dots\dots\dots (17b)$$

Similarly uncoupling equation (16) into two

$$-a \frac{\partial^2 H_\phi}{\partial x^2} = \beta \left(\frac{\partial^2 H_\phi}{a^2 \partial \phi^2} + \frac{\partial p_\phi}{\partial \phi} + a \frac{\partial p_x}{\partial x} \right) \dots\dots (18a)$$

$$\frac{\partial^2 H_\phi}{a^2 \partial \phi^2} = (1-\beta) \left(\frac{\partial^2 H_\phi}{a^2 \partial \phi^2} + \frac{\partial p_\phi}{\partial \phi} + a \frac{\partial p_x}{\partial x} \right) \dots\dots (18b)$$

In this uncoupling process, the terms $\frac{H_\phi}{a}$, and $\frac{\partial^2 H_\phi}{a^2 \partial \phi^2}$ in equations (17) and (18), have been kept on right-hand side and assumed as the loading terms.

As H_ϕ and H_ϕ are the internal forces, one may argue that the uncoupling should be

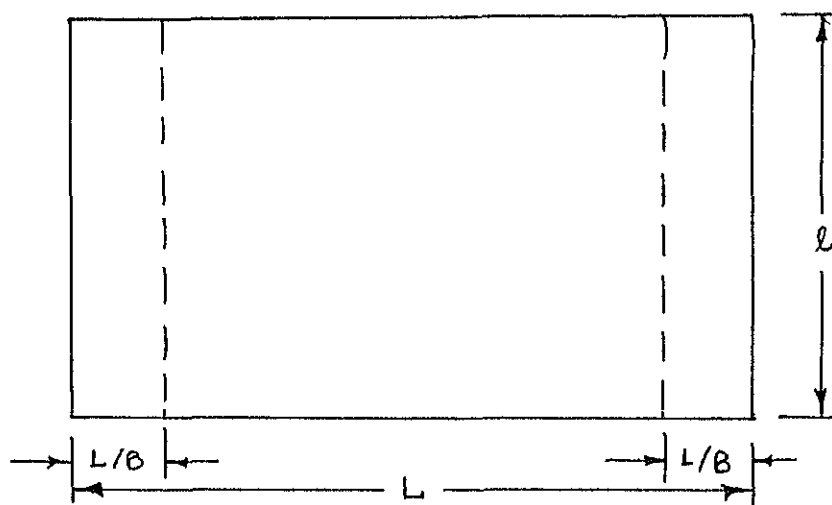
$$\frac{\partial^2 H_\phi}{\partial x^2} = -\alpha p_z$$

$$\text{and } \frac{\partial^2 H_\phi}{a^2 \partial \phi^2} + \frac{H_\phi}{a} = (1-\alpha) p_z$$

This sort of process was tried but the differential equations thus obtained for H_ϕ were identically equal to zero in both regions i.e. on either sides of discontinuity line and hence this was abandoned.

As an example of the use of the above set of equations, a single cylindrical shell roof simply supported on all four edges is designed for a uniformly distributed vertical load. The plan-form of the shell is shown in Figure 25. For simplicity sake, the lines of stress-discontinuity are assumed as shown in Figure 26. It is realized that these lines of discontinuity will not truly represent the load-dispersion in the

two mutually perpendicular directions.



Dotted lines = Stress-discontinuity line

Firm Lines = All sides simply supported side AD roller supported

Figure 25

Substituting the values of α and β for REGION II, the four equations (17,18) reduce to

$$\frac{\partial^2 \phi}{\partial x^2} = 0 \quad \dots(19a)$$

$$\frac{\partial^2 \phi}{\partial y^2} = - \left(\frac{\pi^2}{a^2} + \frac{b^2}{z^2} \right) \quad \dots(19b)$$

$$\frac{\partial^2 \phi}{\partial x^2} = 0 \quad \dots(19c)$$

$$\frac{\partial^2 \phi}{\partial y^2} = \frac{\partial^2 \phi}{\partial x^2} + \frac{\partial^2 \phi}{\partial z^2} + \frac{\partial^2 \phi}{\partial t^2} \dots\dots (19d)$$

and substituting the values of α and β for REGION I, the four equations reduce to

$$\frac{\partial^2 u_z}{\partial x^2} = - \left(\frac{H \phi}{a} + p_z \right) \quad \dots(20a)$$

$$\frac{\partial^2 u_\phi}{\partial \phi^2} = 0 \quad \dots(20b)$$

$$-a \frac{\partial^2 u_z}{\partial x^2} = \frac{\partial^2 u_\phi}{\partial \phi^2} + \frac{\partial p_\phi}{\partial \phi} + a \frac{\partial p_z}{\partial z} \quad \dots(20c)$$

$$\frac{\partial^2 u_\phi}{\partial \phi^2} = 0 \quad \dots(20d)$$

For uniformly distributed load 'p' over whole cylindrical shell surface as shown in Figure 26

$$p_z = p \cos \phi$$

$$p_\phi = p \sin \phi$$

$$p_x = 0$$

Figure 26

substituting this in equations set(20),
we get, for REGION I

$$\frac{\partial^2 u_z}{\partial x^2} = - \left(\frac{H \phi}{a} + p \cos \phi \right) \quad \dots(21a)$$

$$\frac{\partial^2 u_\phi}{\partial \phi^2} = 0 \quad \dots(21b)$$

$$\frac{\partial^2 u_z}{\partial x^2} = - \frac{H}{a} \cos \phi \quad \dots(21c)$$

$$\text{and } \frac{\partial^2 u_\phi}{\partial \phi^2} = 0 \quad \dots(21d)$$

substituting the values of p_z , p_ϕ and p_x in equations set(19)
we get, for REGION II

$$\frac{\partial^2 u_\phi}{\partial x^2} = 0 \quad \dots(22a)$$

$$\frac{\partial^2 u_\phi}{\partial x \partial \phi} = - \left(\frac{u_\phi}{a} + p \cos \phi \right) \quad \dots(22b)$$

$$\frac{\partial^2 u_\phi}{\partial \phi^2} = 0 \quad \dots(22c)$$

$$\frac{\partial^2 u_\phi}{\partial x \partial \phi} = - \frac{1}{a} \phi \quad \dots(22d)$$

Solution of equations-set(21) for REGION I:-

The equations are

$$\frac{\partial^2 u_\phi}{\partial x^2} = - \left(\frac{u_\phi}{a} + p \cos \phi \right) \quad \dots(21a)$$

$$\frac{\partial^2 u_\phi}{\partial x \partial \phi} = 0 \quad \dots(21b)$$

$$\frac{\partial^2 u_\phi}{\partial \phi^2} = - \frac{p}{a} \cos \phi \quad \dots(21c)$$

and $\frac{\partial^2 u_\phi}{\partial \phi^2} = 0 \quad \dots(21d)$

Taking equation (21b),

$$\frac{\partial^2 u_\phi}{\partial x \partial \phi} = 0$$

or $\frac{\partial^2 u_\phi}{\partial \phi^2} = 0$

Integrating twice with respect to ϕ , one gets

$$u_\phi = c_1 \phi + c_2$$

Boundary Conditions:

$$\text{At } \phi = -\phi_0, \quad \psi = 0 \quad \therefore -C_2\phi_0 + C_3 = 0$$

$$\text{At } \phi = +\phi_0, \quad \psi = 0 \quad \therefore C_2\phi_0 + C_3 = 0$$

This gives $C_2 = 0$, $C_3 = 0$

$$\therefore \psi = 0$$

Taking equation (21d),

$$\frac{\partial^2 \psi}{\partial \phi^2} = 0$$

$$\text{or } \frac{\partial^2 \psi}{\partial \phi^2} = 0$$

Integrating twice with respect to ϕ , one gets

$$\psi = C_3\phi + C_4$$

As the load in REGION I is dispersed in x-direction only,

ψ will be equal to zero at $\phi = \phi_0$ and $\phi = -\phi_0$

$$\therefore C_3 = 0 \text{ and } C_4 = 0$$

and hence $\psi = 0$

Taking equation (21e),

$$\frac{\partial^2 \psi}{\partial x^2} = -\frac{P}{a} \cos \phi$$

Integrating twice with respect to x , one gets

$$\psi_x = -\frac{P}{a} \cos \phi \cdot \frac{x^2}{2} + C_5x + C_6$$

Boundary Conditions:

$$\text{At } x=0, \quad \psi_x = 0 \quad \therefore C_6 = 0$$

Therefore

$$\Pi_x = - \frac{p}{a} \cos \phi \cdot \frac{x^2}{2} + C_6 x$$

Using equation (11a),

$$\frac{\partial^2 \Pi_x}{\partial x^2} = - p \cos \phi - \frac{1}{C}$$

Substituting the value of $\Pi_\phi = 0$

$$\frac{\partial^2 \Pi_x}{\partial x^2} = - p \cos \phi$$

Integrating twice with respect to x , one gets

$$\Pi_x = - p \cos \phi \frac{x^2}{2} + C_7 x + C_8$$

Boundary Conditions:

$$\text{at } x = 0, \Pi_x = 0 \therefore C_8 = 0$$

Therefore

$$\Pi_x = - p \cos \phi \frac{x^2}{2} + C_7 x$$

Solution of equations- set (22) for REGION II:

The equations are

$$\frac{\partial^2 \Pi_x}{\partial x^2} = 0 \quad \dots(22a)$$

$$\frac{\partial^2 \Pi_\phi}{a^2 \partial \phi^2} = - \left(\frac{\Pi_\phi}{a} + p \cos \phi \right) \quad \dots(22b)$$

$$\frac{\partial^2 \Pi_x}{\partial x^2} = 0 \quad \dots(22c)$$

$$\frac{\partial^2 \Pi_\phi}{a^2 \partial \phi^2} = - \frac{\Pi_\phi}{a} \quad \dots(22d)$$

Taking equation (11a)

$$\frac{\partial^2 u}{\partial x^2} = 0$$

Integrating once with respect to x , one gets

$$\frac{\partial u}{\partial x} = C_0$$

Due to the symmetry in geometry of the cylindrical shell and the loading, $\frac{\partial u}{\partial x}$ will be equal to zero at $x = L/2$, therefore $C_0 = 0$, therefore $\frac{\partial u}{\partial x} = 0$

Integrating once again with respect to x , one gets

$$u = C_{10}$$

Taking equation (11c),

$$\frac{\partial^2 u}{\partial x^2} = 0$$

Integrating once with respect to x , one gets

$$\frac{\partial u}{\partial x} = C_{11}$$

Due to the symmetry in geometry of the cylindrical shell and the loading, $\frac{\partial u}{\partial x}$ will be equal to zero at $x = L/2$, therefore $C_{11} = 0$, therefore $\frac{\partial u}{\partial x} = 0$

Integrating once again with respect to x , one gets

$$u = C_{12}$$

Taking equation (11d),

$$\frac{\partial^2 u}{\partial \phi^2} = - \frac{u}{R^2}$$

or
$$\frac{\partial^2 H_\phi}{\partial \phi^2} = - H_\phi$$

Its solution is

$$H_\phi = C_{13} \cos \phi$$

As the load in region II is dispersed in ϕ - direction only, an arc-like strip of unit width (in x - direction) can be assumed. This strip shall be under the effect of a vertically down-ward load 'p' per unit of curved length. To avoid any horizontal reaction at the longitudinal edges, one of the two hinged supports is assumed to be a roller support, figure (20).

The strip shall not be subjected to any shear force at any point on either of the side faces because N_x and M_x are constant along x - direction in region II.

Vertical reaction at $\phi = \phi_0$ will be

$$V = p \cdot a \phi_0$$

and its component along the tangent to the curve at $\phi = \phi_0$ will be

$$H_{\phi_0} = p \cdot a \cdot \phi_0 \cdot \sin \phi_0$$

As H_ϕ is given by $C_{13} \cos \phi$, at $\phi = \phi_0$

$$H_{\phi_0} = C_{13} \cos \phi_0$$

Equating it to $p \cdot a \cdot \phi_0 \cdot \sin \phi_0$, one gets

$$C_{13} = p \cdot a \cdot \phi_0 \tan \phi_0$$

Therefore

$$H_\phi = p \cdot a \cdot \phi_0 \tan \phi_0 \cos \phi$$

Taking equation (22b)

$$\frac{\partial^2 u}{\partial \phi^2} = - \frac{u}{a} - p \cos \phi$$

Substituting the value of u_ϕ in the above equation one gets

$$\begin{aligned} \frac{\partial^2 u}{\partial \phi^2} &= - \frac{p \cos \phi \tan \phi_c \cos \phi}{a} - p \cos \phi \\ &= - p (\phi_c \tan \phi_c + 1) \cos \phi \end{aligned}$$

Integrating twice with respect to ϕ , one gets

$$u_\phi = + p a^2 (\phi_c \tan \phi_c + 1) \cos \phi$$

To evaluate the constants, C_6, C_7, C_{10} and C_{12}

In REGION I :-

$$u_x = - \frac{p}{a} \cos \phi \cdot x^2/2 + C_6 x$$

$$\frac{\partial u}{\partial x} = - \frac{p}{a} \cos \phi \cdot x + C_6$$

$$u_x = - p \cos \phi \cdot x^2/2 + C_7 x$$

$$\frac{\partial u}{\partial x} = - p \cos \phi \cdot x + C_7$$

At $x = L/8$

$$u_x)_1 = - \frac{p}{a} \cos \phi \cdot L^2/128 + C_6 L/8$$

$$\left(\frac{\partial u}{\partial x} \right)_1 = - \frac{p}{a} \cos \phi L/8 + C_6$$

$$u_x)_1 = - p \cos \phi L^2/128 + C_7 L/8$$

$$\left(\frac{\partial u}{\partial x} \right)_1 = - p \cos \phi L/8 + C_7$$

In REGION II:-

$$U_x = C_{12}$$

$$\frac{\partial U_x}{\partial x} = 0$$

$$U_x = C_{10}$$

$$\frac{\partial U_x}{\partial x} = 0$$

At $x = L/2$

$$U_x)_2 = C_{12}$$

$$\frac{\partial U_x}{\partial x})_2 = 0$$

$$U_x)_2 = C_{10}$$

$$\frac{\partial U_x}{\partial x})_2 = 0$$

Equating $U_x)_1$, $\frac{\partial U_x}{\partial x})_1$, $U_x)_1$ and $\frac{\partial U_x}{\partial x})_1$ to

$$U_x)_2$$
, $\frac{\partial U_x}{\partial x})_2$, $U_x)_2$ and $\frac{\partial U_x}{\partial x})_2$

From $\frac{\partial U_x}{\partial x})_1 = \frac{\partial U_x}{\partial x})_2$, one gets

$$-\frac{1}{2} \cos \theta \cdot L/2 + C_1 = 0$$

$$\therefore C_1 = \frac{1}{2} \cos \theta \cdot L/2$$

From $U_x)_1 = U_x)_2$, one gets

$$-\frac{1}{2} \cos \theta \cdot L/2 + C_1 \cdot L/2 = C_{12}$$

$$\text{or } C_{10} = \frac{p}{4} \cos \phi \cdot 7L^2 / 128$$

$$\text{from } \left(\frac{\partial \bar{u}_x}{\partial x} \right)_1 = \left(\frac{\partial \bar{u}_x}{\partial x} \right)_2, \text{ one gets}$$

$$- p \cos \phi L/8 + C_7 = 0$$

$$\text{or } C_7 = p \cos \phi L/8$$

$$\text{from } \left(\bar{u}_x \right)_1 = \left(\bar{u}_x \right)_2$$

$$- p \cos \phi L^2 / 128 + C_7 \cdot L/8 = C_{10}$$

$$\text{or } C_{10} = p \cos \phi L^2 / 128$$

Thus, finally one has:

In REGION I,

$$M_x = p/a \cos \phi x/2 \quad (L/4-x)$$

$$M_\phi = 0$$

$$M_x = p \cos x/2 \quad (L/4-x)$$

$$M_\phi = 0$$

and in REGION II

$$M_x = p/a \cos \phi \cdot 7L^2 / 128$$

$$M_\phi = p a \theta_c \tan \theta_c \cos \phi$$

$$M_x = p \cos \phi L^2 / 128$$

$$M_\phi = p a^2 (\theta_c \tan \theta_c + 1) \cos \phi$$

Once the values of M_x , M_ϕ , N_ϕ and N_x are known at different points on the cylindrical shell surface, the reinforcement can be designed by the ultimate strength design procedure as follows:

Assuming the balanced failure, the neutral axis is given by,

$$\eta = \frac{\epsilon_u}{\epsilon_u + \epsilon_{su}} d$$

$$C_u = \frac{2}{3} \sigma_{cu} b k_1 n + A_{sc} (f_{su} - \frac{2}{3} \sigma_{cu})$$

$$-u = A_{st} \sigma_{sy}$$

The external compressive membrane force U will be given as,

$$\begin{aligned} U &= C_u - 2u \\ &= \frac{2}{3} \sigma_{cu} b k_1 n + A_{sc} (f_{su} - \frac{2}{3} \sigma_{cu}) - A_{st} \sigma_{sy} \quad (1) \end{aligned}$$

The external bending moment will be given as,

$$M = \frac{2}{3} \sigma_{cu} b k_1 n (d - 0.5 k_1 n) + A_{sc} f_{su} (d - d_o)$$

In the expressions for M and U , the only unknowns are A_{sc} and A_{st} which can be easily evaluated.

If the membrane force ' U ' is tensile besides the bending moment M , the procedure will be as follows:-

Total steel area needed $A_T = M/f_{su}$ assuming that the section does not take any tension, from the steel beam theory

$$A_{sc} = M/f_{su} (d - d_o)$$

$$\text{and } A_{st} = A_T - A_{sc}$$

CHAPTER VI

CONCLUSIONS AND RECOMMENDATIONS

(a) The procedure for the design of reinforcement in folded plate structures proposed by Suryanarayana⁽¹²⁾ is safe as observed through the experiment, discussed in Chapter II, III and IV. Verifying its authenticity by testing one or two more models of the folded plate structures of different sizes and shapes, the procedure can safely be recommended for the design of reinforcement in the folded plate structures.

(b) On the basis of Hillerberg's method⁽⁷⁾ of calculating the design moments as $M_x^* = M_x \pm |M_{xy}|$, Suryanarayana⁽¹²⁾ has used $\sigma_x^* = \sigma_x \pm |\sigma_{xy}|$ for obtaining the design stresses at different points on the folded plate surface. As σ_x and σ_{xy} are not the pure bending stresses, this modification procedure needs more explanation.

For the cylindrical shell structures:

(c) Criterion for the choice of the stress-discontinuity-lines representing more realistic load-dispersion (than that adopted in Article 5.1, Figure 25), needs to be evolved.

(d) It is recommended that a series of experiments should be conducted to study the structural behaviour of the cylindrical shell structures.

(e) From the experimentally observed failure models, an appropriate yield line pattern should be chosen on the cylindrical shell surface and then its ultimate load capacity should be computed by yield line theory.

(f) The comparison of the experimentally observed and the theoretically obtained ultimate strength will prove the authenticity of

the procedure proposed in this dissertation.

- (c) The yield- criterion under the effect of bending and membrane forces needs to be studied before its application in the computation of the ultimate strength of the cylindrical shell structures by yield-line theory.

the procedure proposed in this dissertation.

- (c) The yield- criterion under the effect of bending and membrane forces needs to be studied before its application in the computation of the ultimate strength of the cylindrical shell structures by yield-line theory.

9. Wood, R. H., "The Reinforcement of Slabs in Accordance with a Predetermined Field of Moments", Concrete, vol.2, Number 2, February 1962, pp.60.
10. Crawford, R. E., "Limit Design of Reinforced Concrete Slabs", Ph. D. Thesis, University of Illinois, 1962.
11. Ramaswami, G. S., "Design and Construction of Concrete Shell Roofs" McGraw Hill, pp.
12. Suryanarayana, P., "Rational Design of Folded Plate Structures", M. Tech. Thesis, Department of Civil Engineering, I.I.T. Kanpur, July, 1969.
13. Granholm, H., "A General Flexural Theory of Reinforced Concrete", John Wiley and Sons, New York, pp. 189.

TABLE NO. 2
*Plotted in Fig. 15

Loading Step No. (21.34 psi)	Longitudinal Strain								Lateral Strain							
	Strain Gauge Number								Strain Gauge Number							
	16 ^a	17	18	25 ^a	32	34	20	22	24	26	28	38				
1	27	28	31	5	35	20	0	21	23	-	-227	12				
2	62	68	62	18	73	58	4	51	57	-19	-83	37				
3	105	107	92	39	110	111	10	84	101	-13	-69	68				
4	152	148	139	62	146	150	28	131	155	-	-64	118				
5	184	167	162	78	175	172	25	163	194	-	-57	145				
6	243	223	209	105	233	220	50	206	268	4	-77	188				
7	295	228	237	124	235	252	71	236	295	3	-77	210				
8	327	227	248	143	290	260	89	251	340	-	-108	241				
Time Effect																
9	325	176	172	18	220	156	5	151	277	-89	-180	177				
10	400	216	224	66	282	227	35	218	345	-65	-185	230				
11	447	241	260	120	328	288	60	264	398	-47	-187	284				
12	437	262	361	158	370	277	88	319	426	-32	-171	314				
Time Effect																
13	1024	890	882	628	970	824	780	841	995	655	531	847				
14	1029	908	897	660	993	849	820	876	1039	653	573	879				
15	1067	956	964	698	995	875	835	950	1017	651	601	907				

TABLE NO. 3

* plotted in Fig. 16

Loading Step No.	Lateral Strain (micro inch/ inch)													
	Strain Gauge number													
	30	35	19*	21*	31	36	27*	23*	37	13	14			
1	18	1	8	12	- 6	- 15	- 7	23	- 30	5	14			
2	8	22	10	48	- 22	- 21	- 19	65	- 20	13	47			
3	24	62	11	79	- 14	8	- 22	103	16	33	100			
4	33	86	35	124	- 19	20	- 19	160	49	65	153			
5	48	116	35	138	- 26	23	- 22	204	60	75	189			
6	38	141	65	182	- 28	21	- 11	258	80	108	266			
7	107	151	96	198	- 21	- 18	- 26	310	95	78	356			
8	143	151	105	242	- 21	- 50	- 14	317	126	72	404			
Time Effect														
9	190	66	45	159	- 71	- 160	- 53	210	60	80	414			
10	275	93	72	237	- 53	- 149	- 43	260	120	133	538			
11	398	118	81	322	- 71	- 120	- 28	335	175	161	612			
12	526	123	130	347	- 101	- 85	- 16	390	190	190	704			
Time Effect														
13	1971	361	793	956	536	488	688	914	690	- 9	- 660			
14	2078	376	805	997	559	520	712	945	705	21	- 602			
15	2473	361	865	1040	570	560	712	1013	712	35	- 560			

TABLE NO. 4

(*Average values Plotted in Fig. 17)

Loading Step	Vertical deflection at mid-span (1/10 m m) Edge Beams and Middle Fold											
	Dial Gauge Number											
	2	5	Average*	15	16	Average*	13	18	Average*	14	17	Average*
1	1	2	1.5	12	12	12	4	9	6	15	11	13
2	6	5	5.5	26	27	26.5	9	20	14	27	28	27
3	11	9	10	40	45	42.5	12	31	22	42	44	43
4	18	13	15.5	54	62	58	30	45	37	57	59	56
5	25	18	21.5	70	80	75	46	59	52	74	84	79
6	36	25	30.5	99	112	105.5	62	81	71	101	112	107
7	49	45	47	152	172	162	95	117	106	146	168	157
8	74	62	68	207	230	218	134	153	144	195	224	209
Time Effect												
9	121	91	106	327	357	342	219	226	222	302	340	321
10	142	111	126.5	372	430	391	248	259	253	342	389	365
11	178	139	158.5	437	477	457	301	311	307	402	455	428
12	248	189	218.5	529	575	552	377	388	382	487	551	519
Time Effect												
13	342	229	285	754	820	787	497	547	517	685	793	739
14	377	260	318	812	887	850	532	591	561	737	854	795
15	445	311	378	917	997	957	619	662	640	833	952	892

TABLE NO. 5

(*Average values Plotted in Fig. 18)

Loading Step	Vertical deflections at quarter span (1/10 m m), upper fold										
	Dial Gauge Number										
	7	12	19	24	Average*	8	11	20	23	Average*	
1	7	4	10	6	6	1	6	15	12	8	
2	15	11	27	13	16	12	14	27	22	19	
3	22	19	35	22	23	25	26	39	36	32	
4	32	28	42	32	33	39	35	55	48	44	
5	44	37	55	42	44	54	48	69	62	58	
6	60	52	70	57	60	75	71	90	81	84	
7	82	72	94	80	82	107	98	127	118	110	
8	106	98	117	108	107	146	136	167	152	150	
Time Effect											
9	155	153	155	164	157	215	205	257	221	219	
10	176	173	175	184	177	258	233	274	248	253	
11	207	205	207	218	209	297	272	320	290	295	
12	267	259	250	278	264	361	332	385	350	357	
Time Effect											
13	372	376	335	393	369	-	477	-	490	484	
14	405	408	413	425	413	-	516	-	530	523	
15	455	466	442	494	464	-	585	-	613	599	

TABLE NO. 6

(*Average values Plotted in Fig. 18)

Loading Step (21.34 psf)	Vertical Deflections at quarter span (1/10 in), Edge Beams and Middle Fold											
	Dial Gauge Number											
	1	3	4	6	Average [*]	9	10	21	22	Average [*]		
1	1	1	2	1	1.25	10	5	10	12	9		
2	4	5	5	2	4	22	26	28	22	19.5		
3	8	9	8	8	6.25	34	27	35	33	32		
4	14	14	13	11	13	48	36	50	45	45		
5	20	20	18	18	19	62	50	65	58	59		
6	28	30	28	30	29	85	70	87	78	80		
7	38	41	40	42	40	121	106	132	123	120		
8	55	62	53	55	56	166	149	170	160	161		
Time Effect												
9	94	105	73	63	83	250	232	258	242	245		
10	103	122	65	75	96	283	265	299	269	279		
11	132	146	110	100	122	327	306	350	336	330		
12	178	193	140	145	164	391	368	424	377	390		
Time Effect												
13	259	266	188	198	227	585	532	579	530	557		
14	272	279	196	217	241	639	588	646	576	612		
15	322	334	228	250	283	732	678	741	666	704		

TABLE No. 7

Plotted in Fig. 19

Loading Step	Horizontal Deflections of Edge Beams (1/100 mm)				
	Dial Gauge Number				
	25	26	27	28	29 30
1	5	3	3	7	7
2	9	3	5	14	15
3	16	10	11	22	24
4	22	18	18	32	35
5	30	23	20	43	47
6	41	32	25	-	62
7	52	45	30	43.5	74
8	56	60	38	52	85
Time Effect					
9	67	75	23	116	118
10	68	90	30	126	135
11	77	102	33	134	160
12	91	115	40	153	195
Time Effect					
13	82	59	7	- 21	114
14	84	64	41	- 10.5	122
15	-116	67	45	4	132

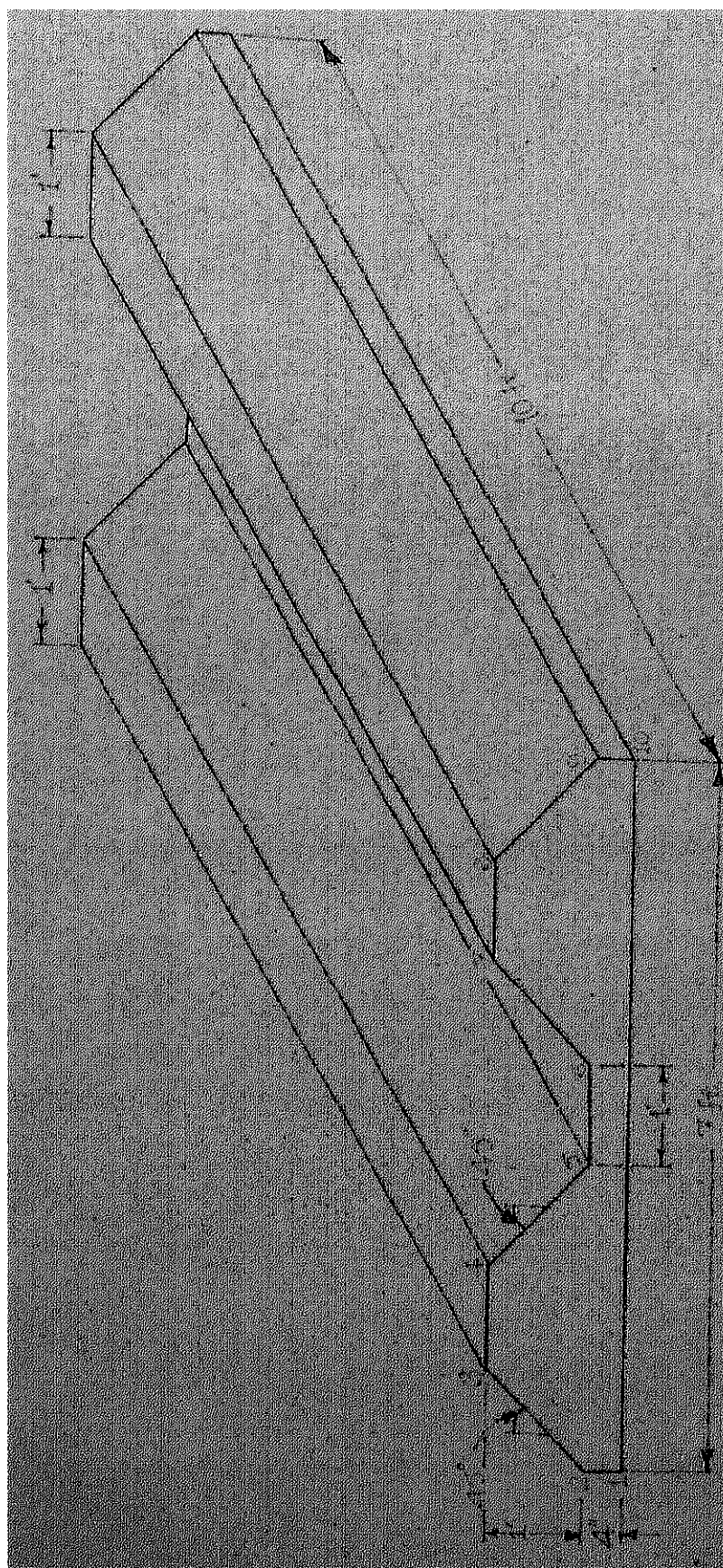


FIG. 1 ISOMETRIC VIEW OF FOLDED PLATE MODEL
WITH DIMENSIONS

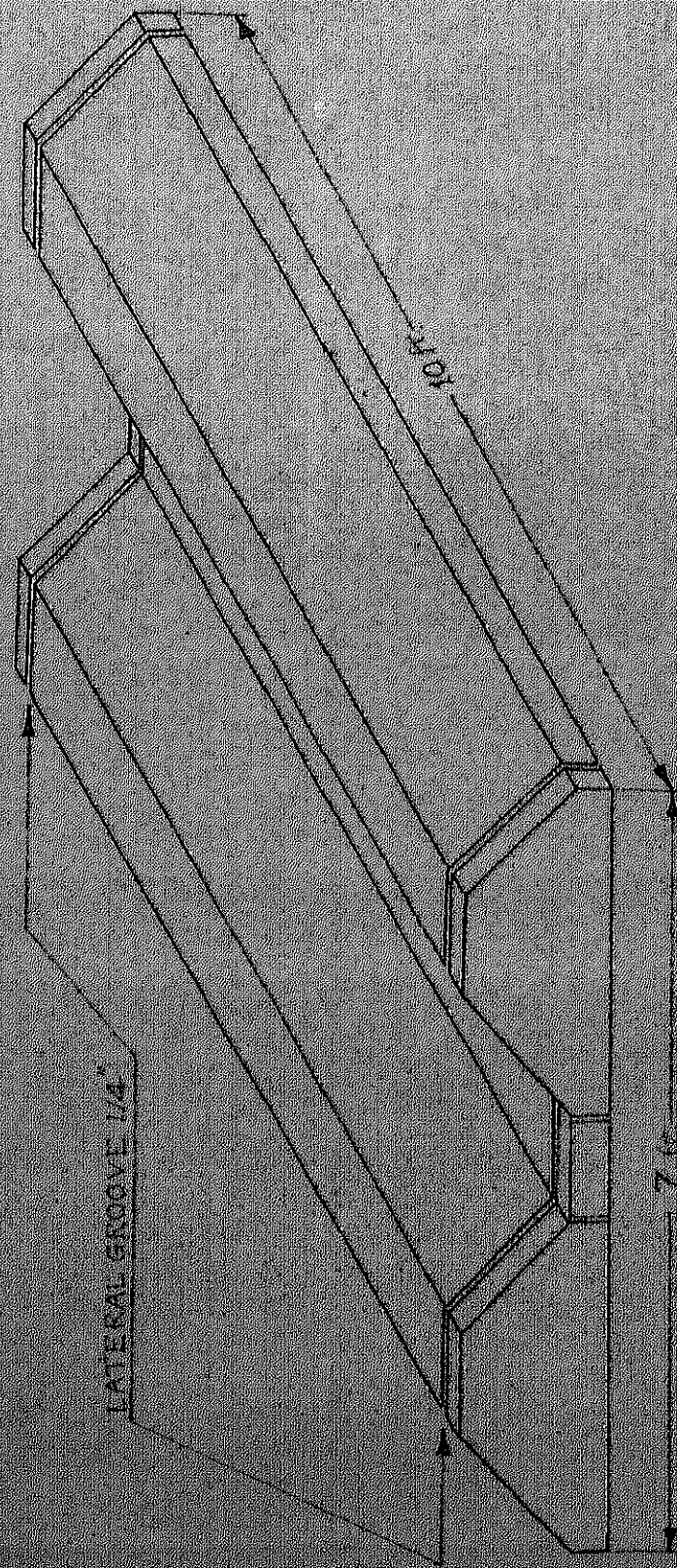


FIG. 2. ISOMETRIC VIEW OF INTERIOR FORM WORK WITH $\frac{1}{4}$ " GROOVE

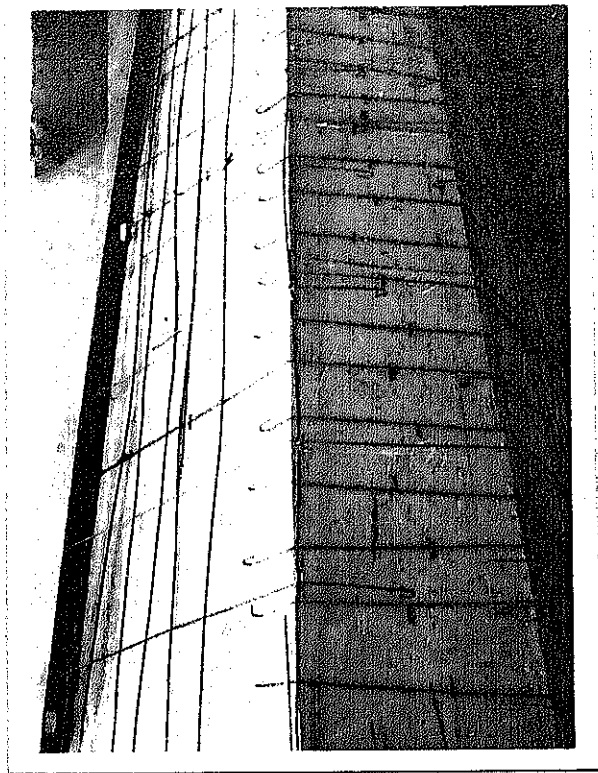


FIG. 3

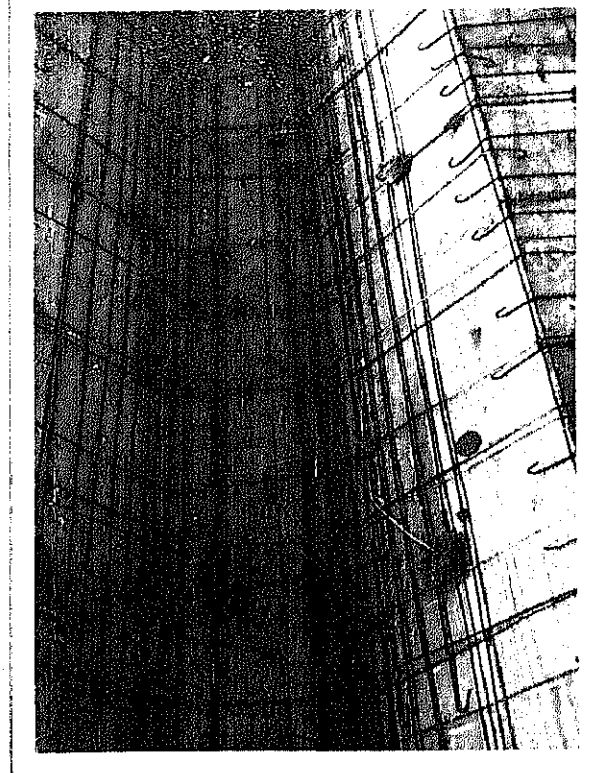


FIG. 4

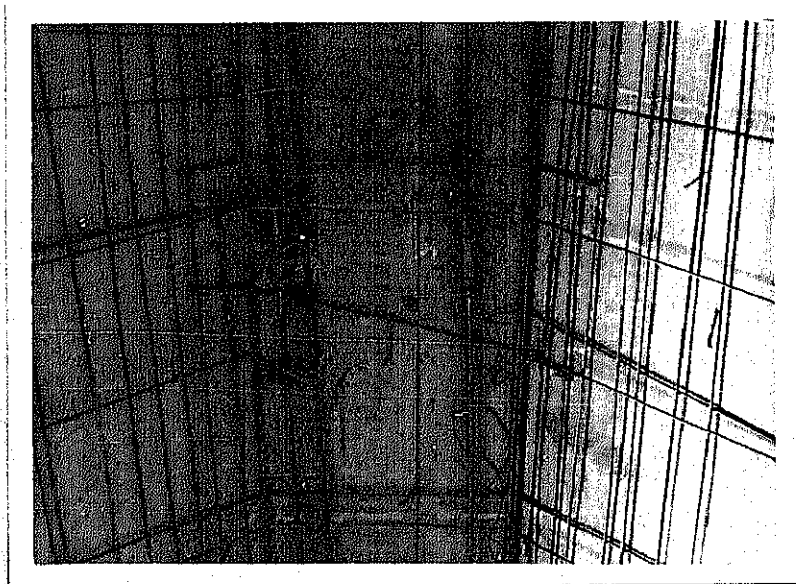


FIG. 5

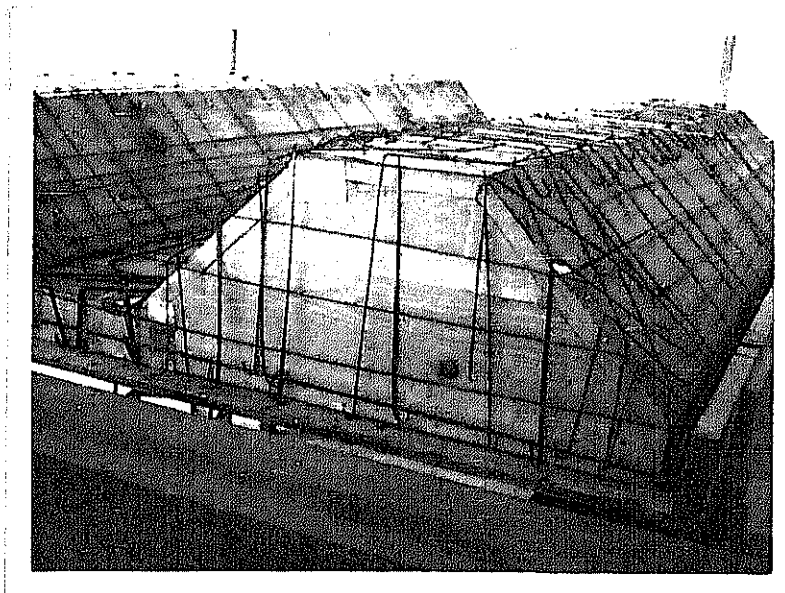


FIG. 6

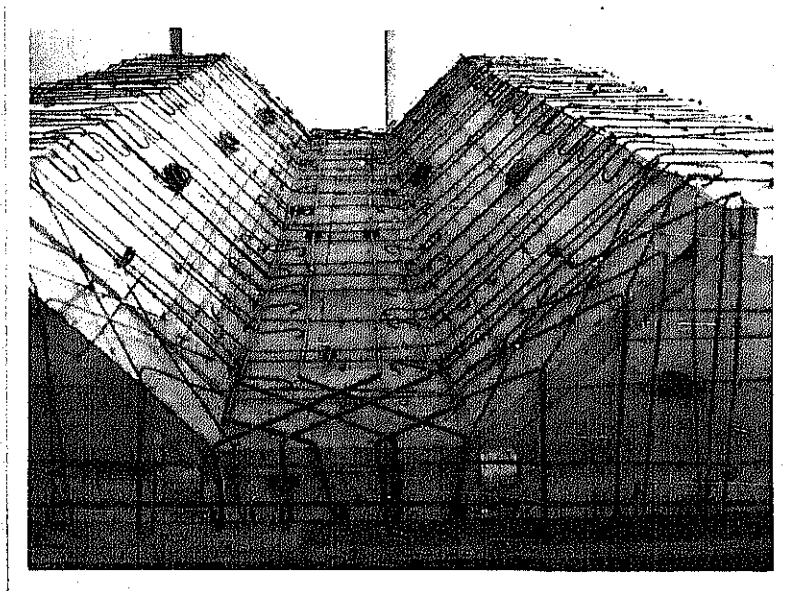
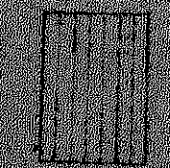
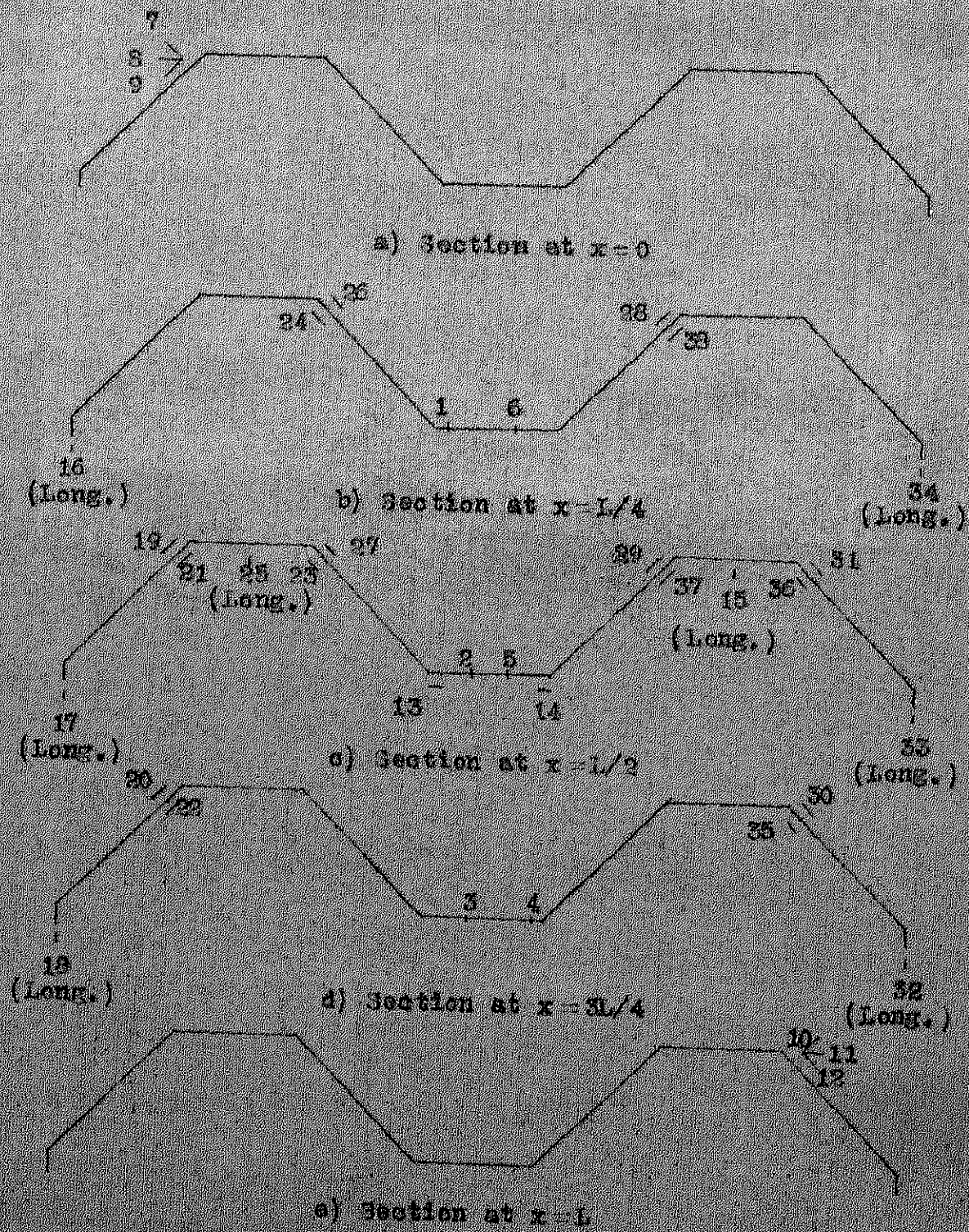
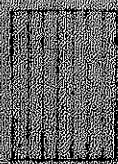
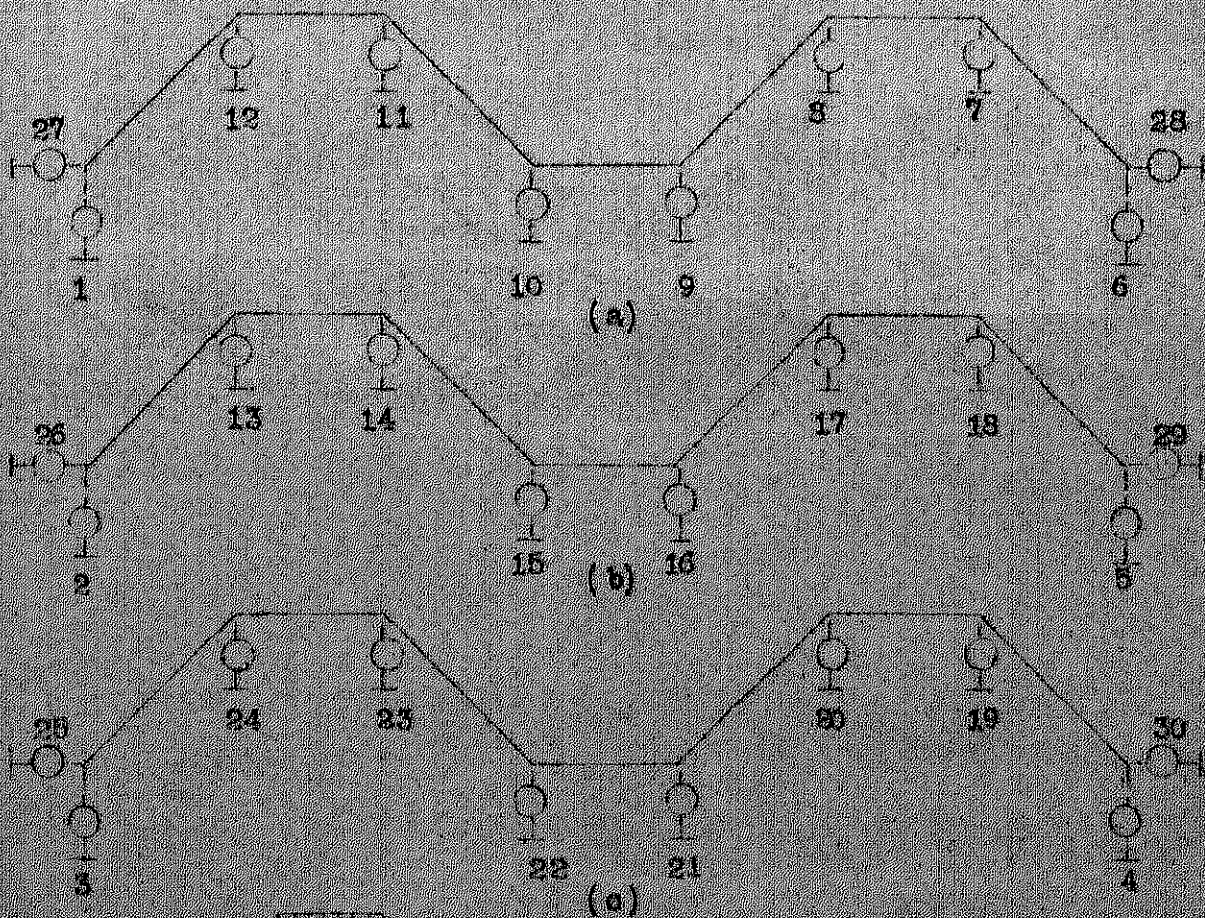


FIG. 7



Key plan

FIG. 8. LOCATION OF THE STRAIN GAUGES ON THE MODEL



Key plan

- (a) Section at $x=L/4$
- (b) Section at $x=L/2$
- (c) Section at $x=3L/4$

FIG. 9. LOCATION OF THE DIAL GAUGES ON THE MODEL



FIG. 10



FIG. 11

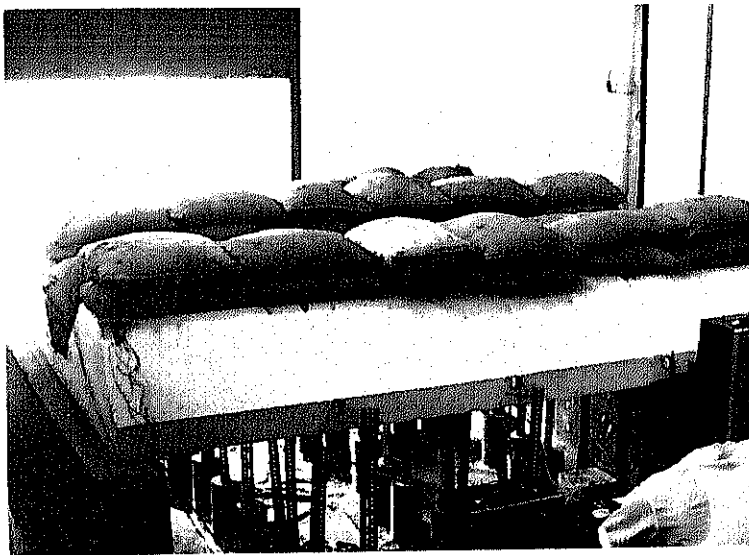


FIG. 12

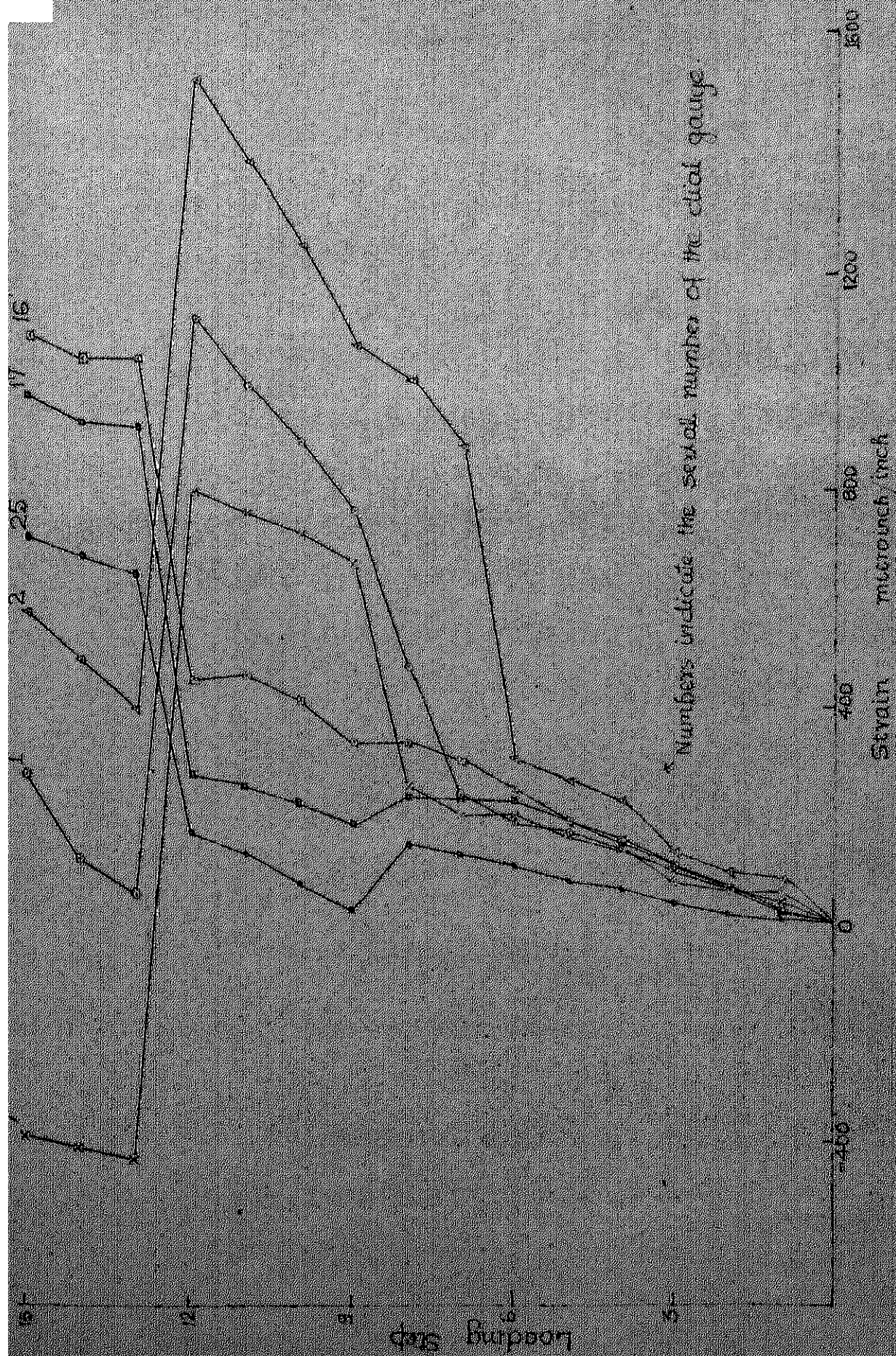


FIG. 15 LOAD VS LONGITUDINAL STRAIN

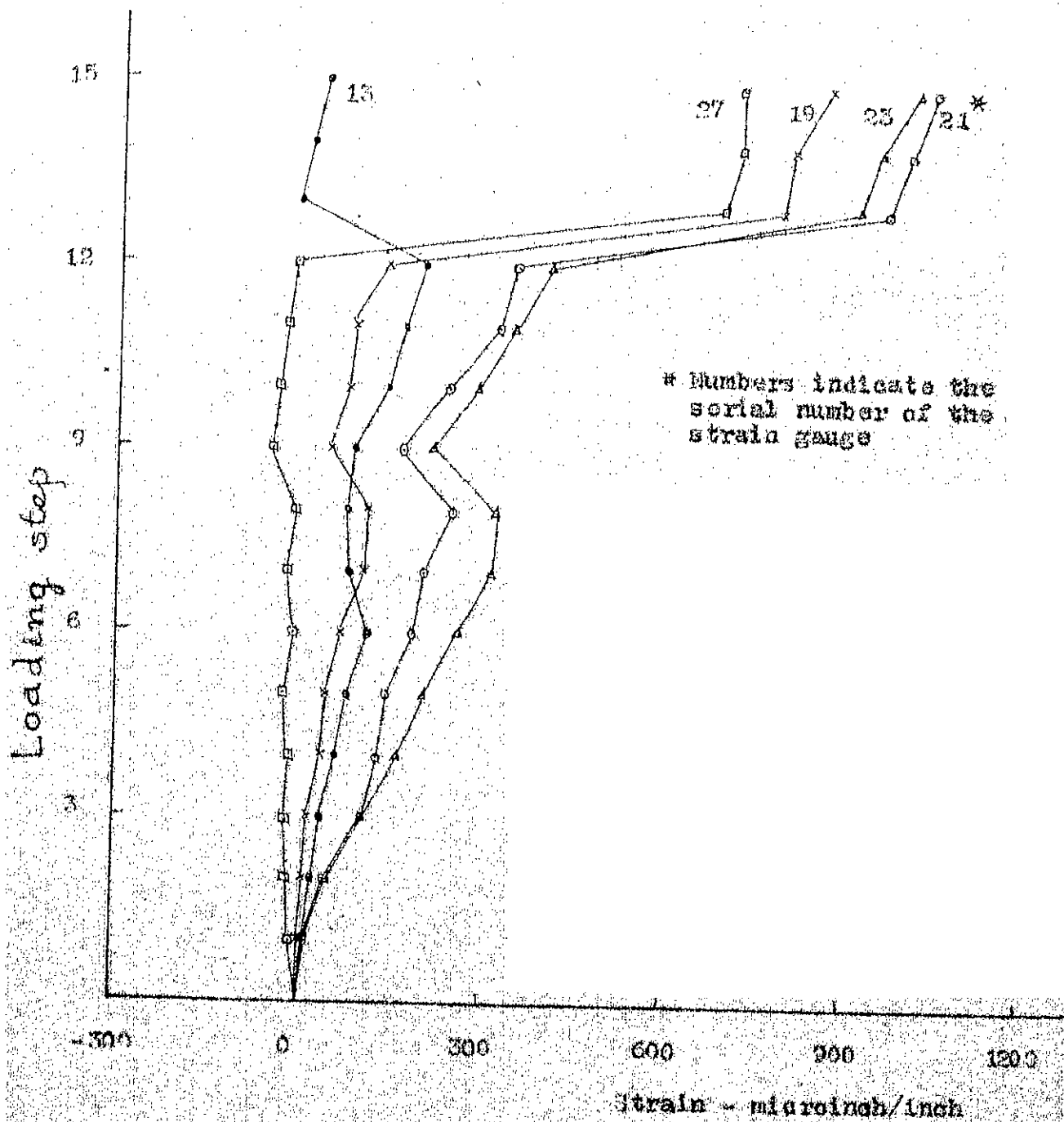
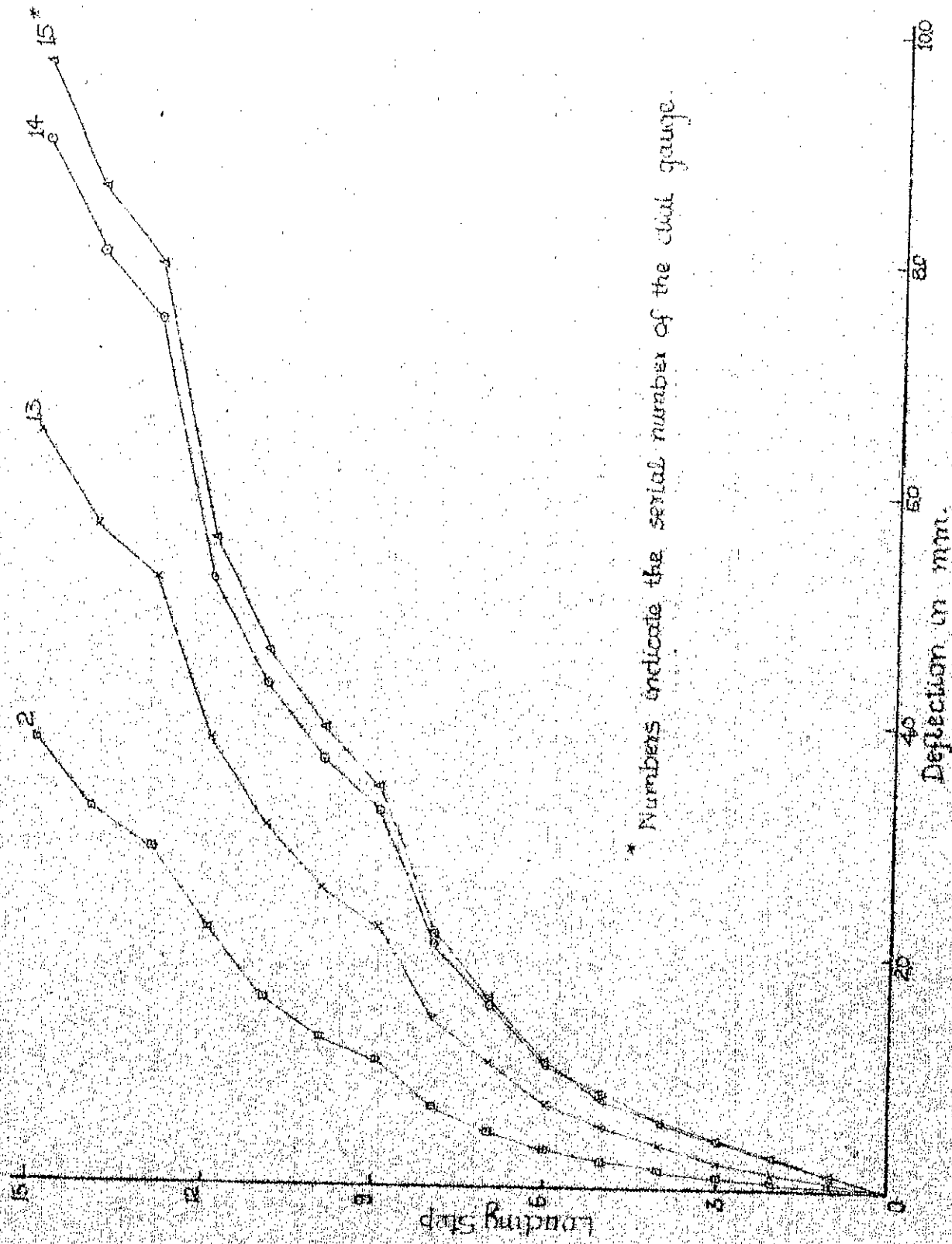
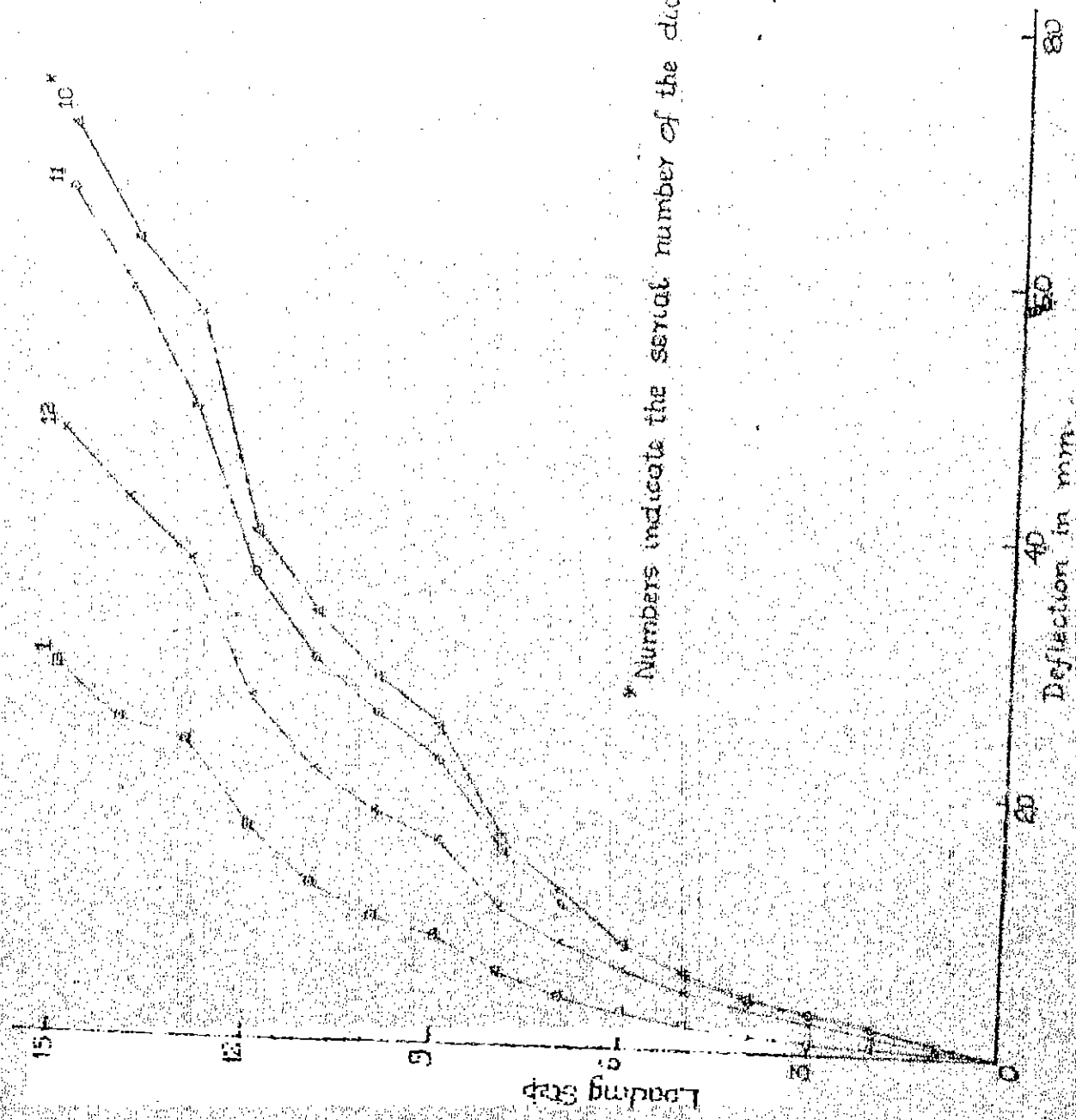


FIG. 16. LOAD vs LATERAL STRAIN



* Numbers indicate the serial number of the dial gauge.

FIG. 17 LOAD VS VERTICAL DEFLECTION AT MIDSPAN



* Numbers indicate the serial number of the dial gauge

FIG.16 LOAD VS. VERTICAL DEFLECTION AT QUARTER SPAN

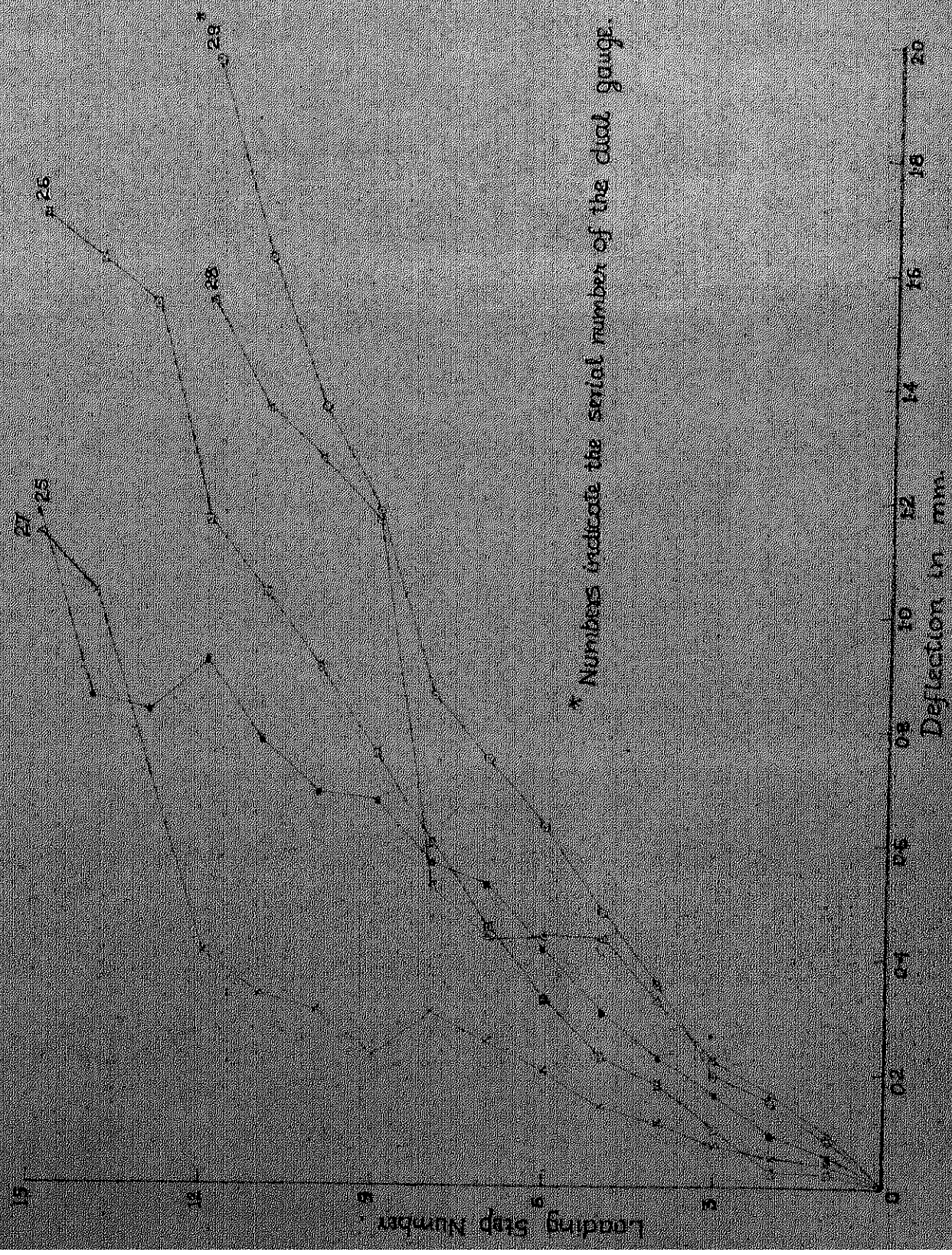


FIG. 19. LOAD VS. HORIZONTAL DEFLECTION OF EDGE BEAMS.

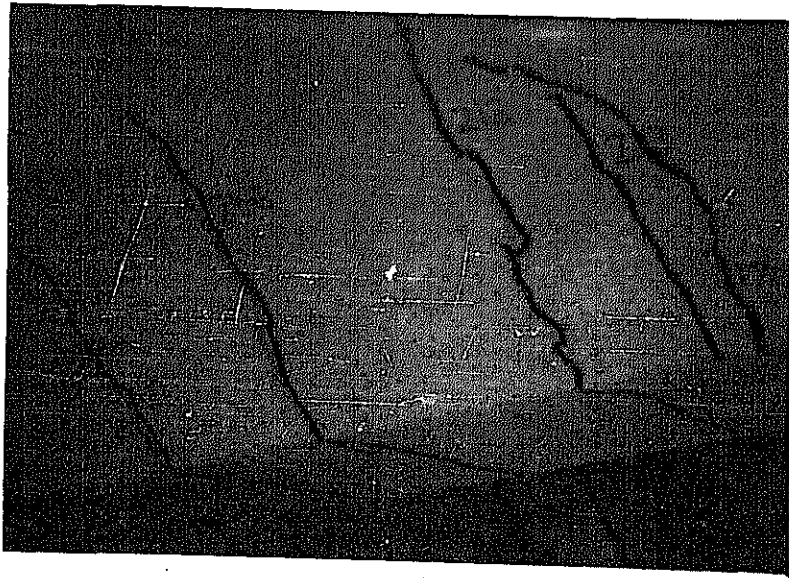


FIG. 20

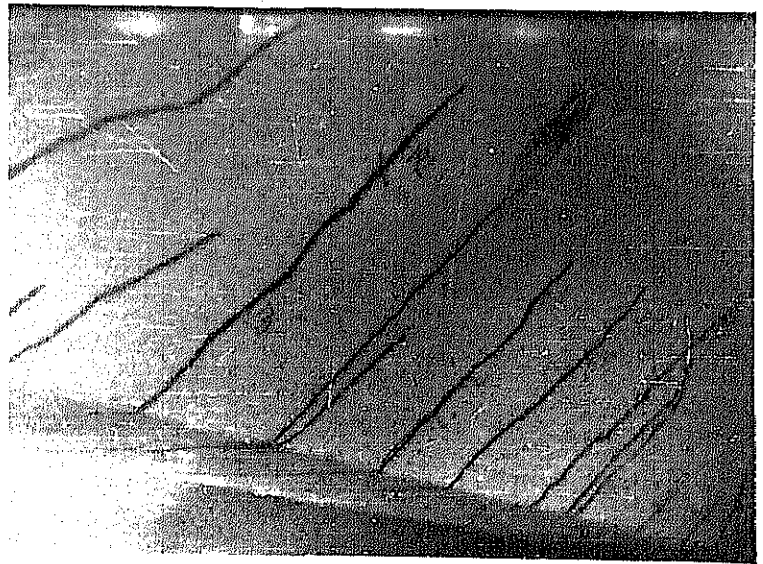


FIG. 21

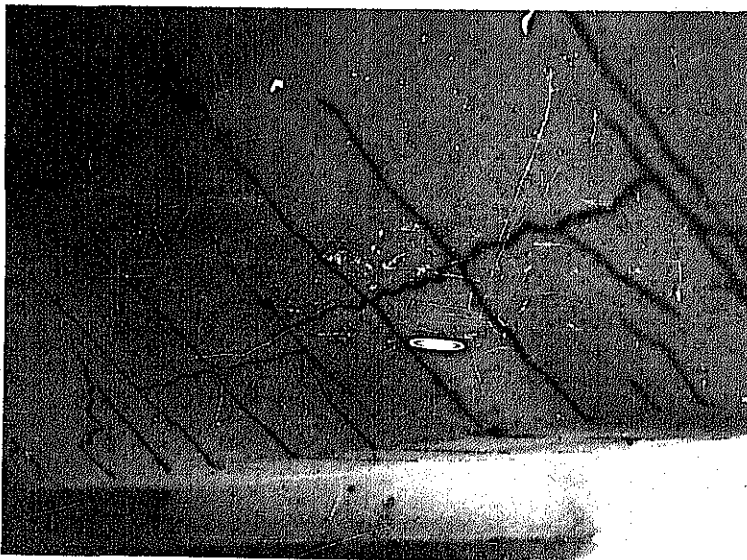


FIG. 22

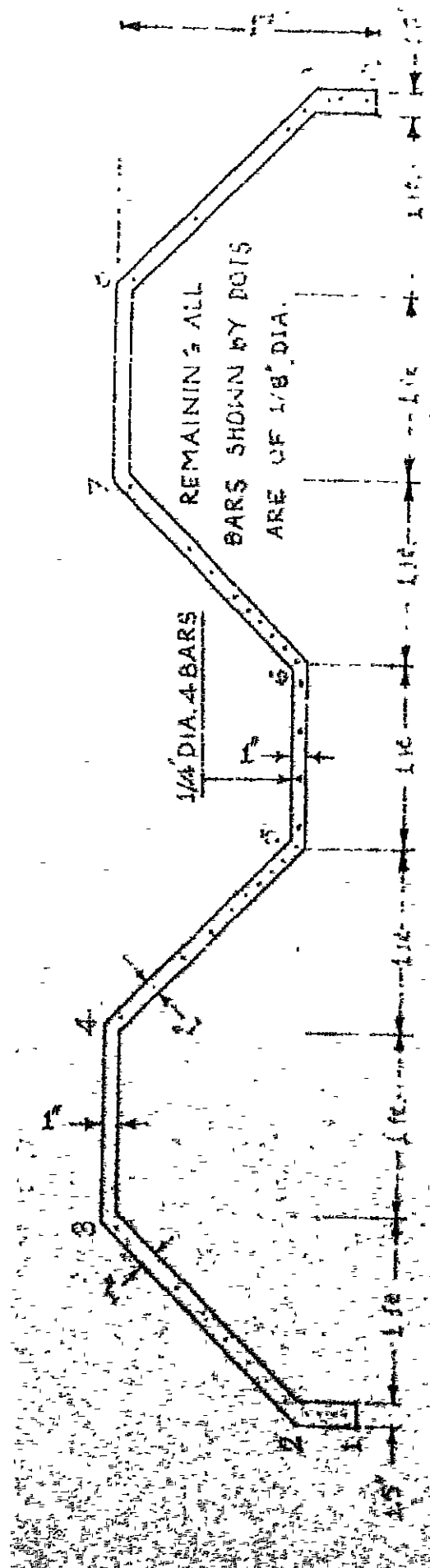


FIG. 23 LONGITUDINAL REINFORCEMENT

AT MID-SECTION

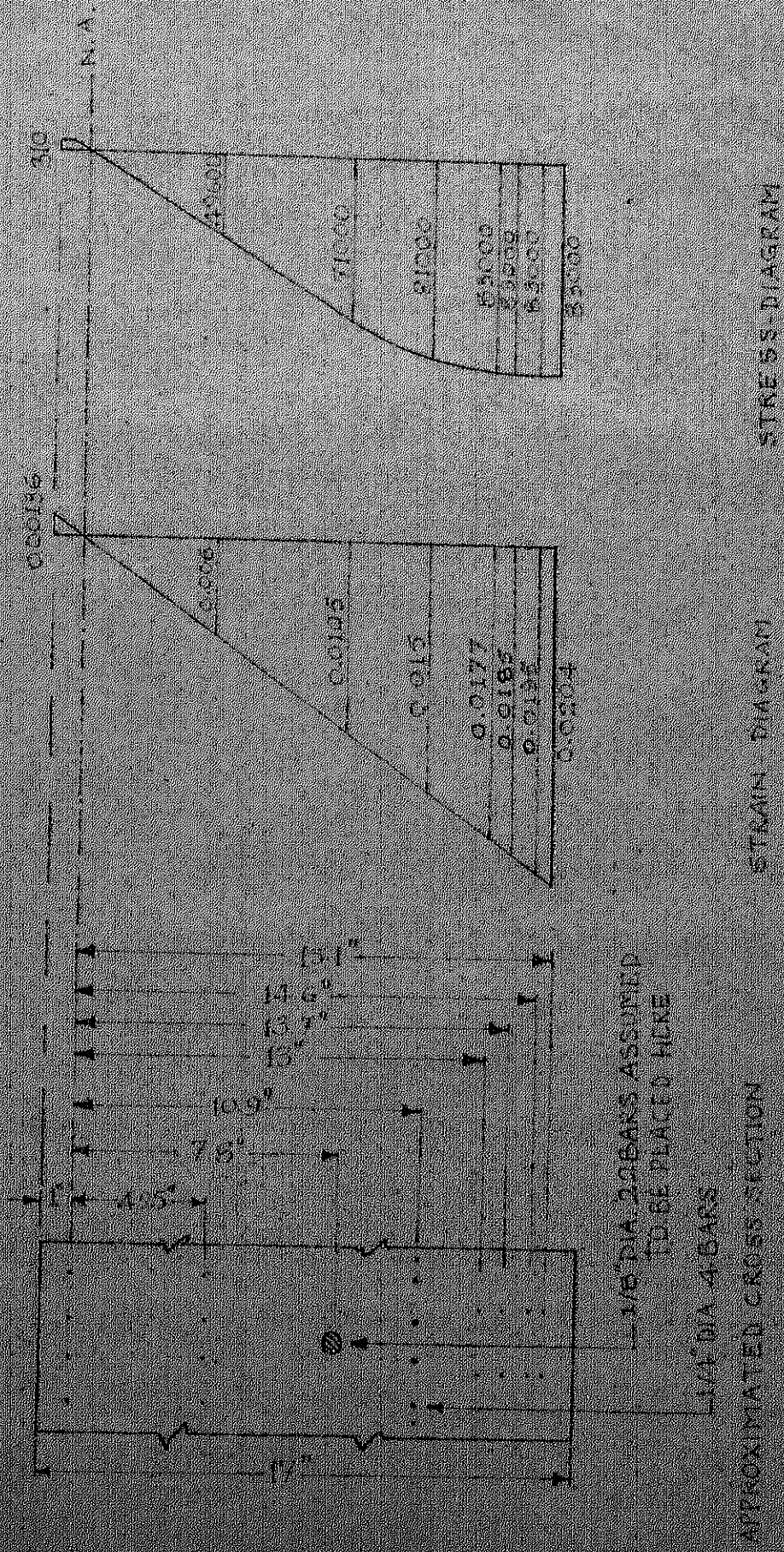


FIG 24.

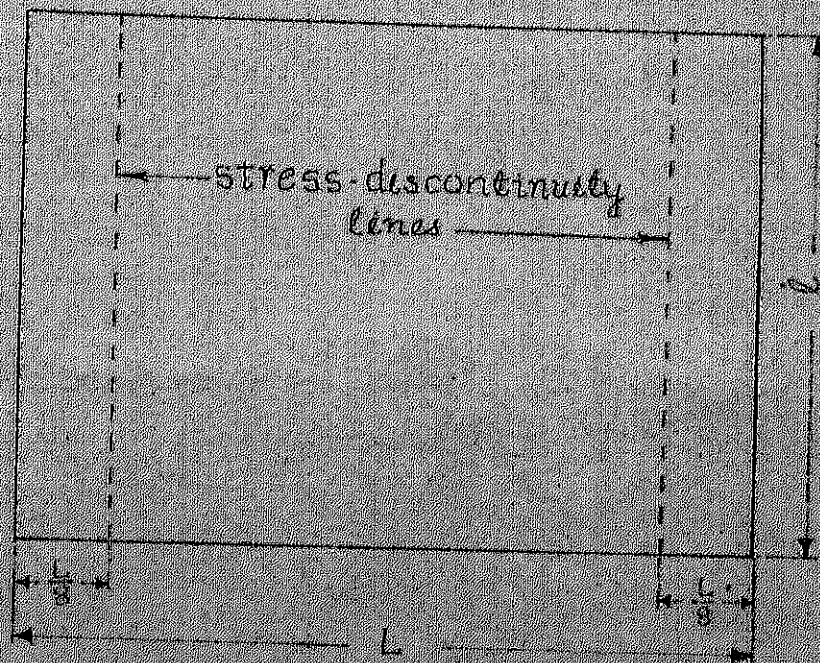


FIG. 25. STRESS-DISCONTINUITY LINES OVER CYLINDRICAL SHELL MODEL IN PLAN

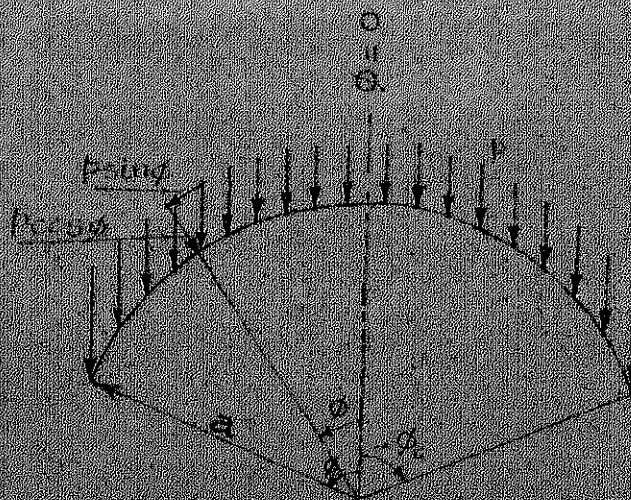


FIG. 26. UNIFORMLY DISTRIBUTED LOAD p AND ANGLE ϕ

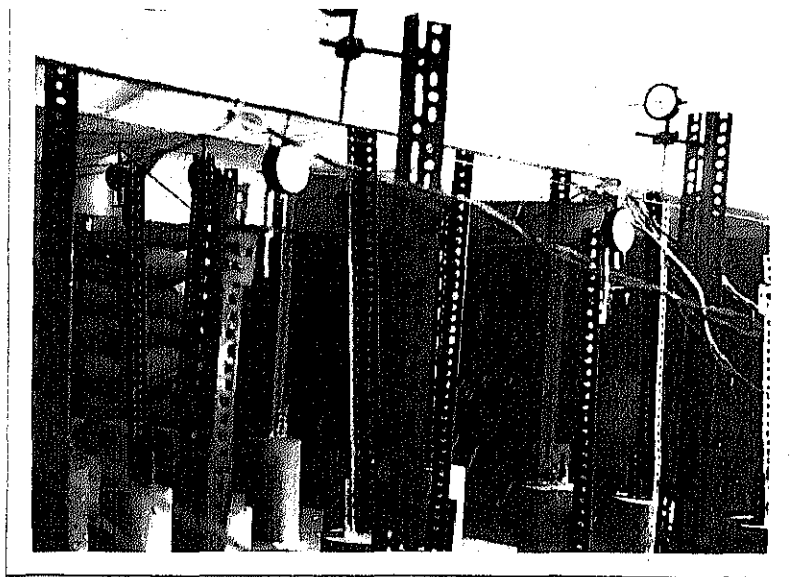
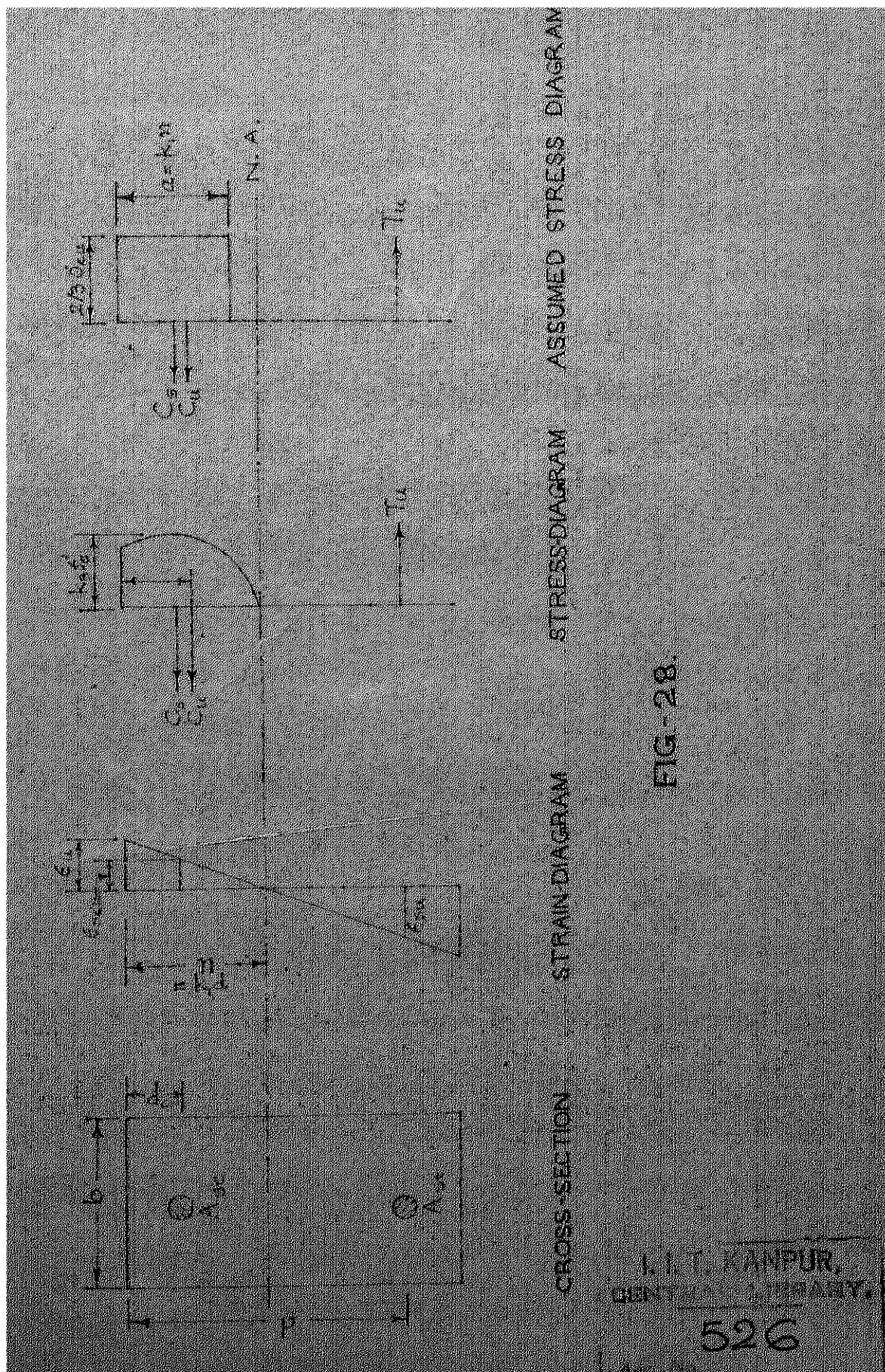


FIG. 27



I. I. T. KANPUR,
CENTRAL LIBRARY.

526

Singh,
Experimental and analytical
study of the design of reinfor-
cement in folded plates and
cylindrical shell structures.